Master's Thesis of Science in Earth and Environmental Sciences

Formation of ice wedges and origin of trapped greenhouse gas at Zyryanka, Northeastern Siberia

시베리아 북동부 지랸카 지역의 얼음 쐐기 형성과 포집된 온실가스 기원

February 2023

Graduate School of Natural Sciences
Seoul National University
Earth and Environmental Sciences Major

Nayeon Ko

Formation of ice wedges and origin of trapped greenhouse gas at Zyryanka, Northeastern Siberia

Adviser Jinho Ahn

Submitting a master's thesis of
Science in Earth and Environmental Sciences
October 2022

Graduate School of Natural Sciences
Seoul National University
Earth and Environmental Sciences Major

Nayeon Ko

Confirming the master's thesis written by
Nayeon Ko
January 2023

Chair _____(Seal)
Vice Chair _____(Seal)
Examiner_____(Seal)

Abstract

Multiple geochemical analyses may help us better constrain the ice-wedge formation process and in-situ greenhouse gas (GHG) production mechanisms. Here I present new results from ice-wedges sampled at Zyryanka, Northeastern Siberia. The plant remains and CO_2 gas in the wedges were analyzed for radiocarbon dating, and I obtained 810-1750 years before 1950 CE for the ice wedges and 4220 years before 1950 CE for the adjacent soils. $\delta(N_2/Ar)$ of the ice wedges ranges from -17.51 to -3.53 % with respect to modern air, indicating that the ice wedge was formed by infilling both liquid water and hoar frost. On the other hand, the $\delta(O_2/Ar)$ value of the Zyryanka ice wedges ranges from -72.88 to -37.58 % with respect to modern air, implying that oxygen gas was selectively consumed by microbial respiration in the ice-wedge ice. Greenhouse gas compositions (CO_2, CH_4 and N_2O) are a few orders of magnitude higher than the Holocene atmospheric levels. Our geochemical and texture analyses show that the greenhouse gas was mostly produced by microbial activity, but partially originated from the dissolved gas in the infilling liquid water. The $\delta^{18}O$ values are -28.14 ± 0.39 and -21.85 ± 1.96 ‰ (mean ± 1σ) for the ice wedge and adjacent soil ice, respectively, implying that isotopic diffusion from soil to ice wedge is negligible. Comparing with the $\delta^{18}O$ value of modern precipitation in the Zyryanka region, it can be inferred that the ice wedge was mainly formed by winter

precipitation (from October to April). This study suggests that the gas mixing ratios in ice wedges and stable water isotope chemistry may help better understanding the biogeochemical environments during and after the formation of ice wedges, as well as verify the reliability of ice wedges as paleoclimate proxies.

Keyword : permafrost, ice-wedge, water stable isotope, greenhouse gas, gas mixing ratios, Northeastern Siberia

Student Number : 2020-28766

Table of Contents

Chapter 1. Introduction

Ice wedges form in thermal-contraction crack polygons (Hugh et al. 2007) at humid permafrost regions by permeation of snow meltwater into the cracks in the spring or by growth of hoarfrost in the open crack in the winter (Robert et al. 1976).

In many studies, water stable isotopes ($\delta^{18}O$ and δD) of ice wedges have been commonly utilized as a proxy for winter climate (e.g., Mackay et al., 1983; Vasil'chuk, 1991; Gibson and Prowse, 2002; Popp et al., 2006; Meyer et al., 2010a, 2010b; Opel et al., 2011; Boereboom et al., 2013; Porter and Opel, 2020; Campbell-Heaton et al., 2021) in contrast with biological proxies such as tree rings, diatoms and pollen data that are exclusively used for the reconstruction of summer climate conditions (Miller et al., 2010; Meyer et al., 2015). On the other hand, deuterium excess (d-excess= $\delta D - 8 \times \delta^{18}O$) reported by Dansgaard (1964) were used to constrain the fractionation process experienced during or after the formation of ice wedge or the change in moisture source conditions (Boereboom et al. 2013; Meyer et al. 2002). Despite the extensively accepted knowledge that ice wedge can be used as a winter climate proxy, it has not been well scrutinized whether they essentially reflect and maintain the isotope chemistry of winter precipitation due to lack of understanding ice wedge formation processes and geochemical environments in ice after the formation.

Previous studies have challenged about the reliability of ice wedges as the paleoclimate proxy due to the alteration of outermost few cm of ice wedges by adjacent host sediments (Meyer et al., 2007; Meyer et al., 2010a; Opel et al., 2011). Meyer et al. (2010a) suggested that these exchange effect may occur 10-15 cm of ice and adjacent soil, respectively. Therefore, it cannot be ruled out the modification of original paleoclimate signal of the ice wedge due to the physicochemical processes. Campbell-Heaton et al. (2021) also reported that it may be challenging to use water isotope records of ice wedges as proxies for paleoclimate

reconstruction due to chemical alterations caused by the physical processes such as infiltration of unfrozen soil water into ice wedge cracks (i.e., edge effect) during or after the formation of ice wedges. In this case it can be observed gradual increase in $\delta^{18}O$ toward the ice wedge margins, which was attributed to increase in moisture at the ice wedge interface. In the same aspects, Galanin (2021) also raises many questions regarding the reliability of ice wedge as a proxy in terms of paleoclimate reconstruction. According to that study, it is argued that more discussion is needed as to whether the ice wedge has not actually undergone significant changes in terms of isotope composition and formation mechanisms. To avoid these limitations, convincing geochemical evidence are required to support that ice wedge was originated from winter precipitation and the isotopic compositions was well preserved. Regarding physical alteration processes, Cardyn et al (2007) proposed that the molar ratio of the inert gas species entrapped in ice can be used to check if ice was formed by dry snow densification or snow meltwater refreezing. The N_2/Ar ratios of ice considerably decrease from the atmospheric value when ice forms by freezing of liquid water which contacted open atmosphere because the gas solubility of N_2 and Ar is different. The N_2/Ar method were used in multiple studies (Kim et al., 2019; Boereboom et al., 2013; Lauriol et al., 2010). However, although N_2/Ar mixing ratio can be used to identify melting status of ice wedge or amount of liquid water contributed to the formation, the ice-wedge formation process have been poorly investigated. For example, if the ice wedge was formed by liquid water mixing with snow, specific information of liquid water types (e.g., snow meltwater, soil water, summer precipitation, ground water, etc.) were not provided. Therefore, further discussion on the ice wedge formation process is required to better identify ice wedge filling materials and to determine the factors that can modify the original chemical compositions of the ice wedge.

Moreover, the environmental conditions at the time of ice wedge development can be inferred by multiple isotopes of ice wedge ice (Boereboom et al., 2013; Opel et al., 2011; St-Jean et al.,

2011; Vasil'chuk et al., 2021). For example, comparison with the regression slope of local meteoric water line (LMWL) to that of ice wedge in the $\delta^{18}O$-δD relationship allows us to determine whether ice wedge was experienced secondary isotopic fractionation during or after its formation (Lacelle, 2011a).

Recently, greenhouse gases (GHGs) occluded in ice wedges draw attention because they may give us additional information of climate and ground environments in the past (Brouchkov and Fukuda, 2002; Boereboom et al., 2013; Kim et al., 2019). Combined with mixing ratio of oxygen and argon ($\delta(O_2/Ar)$), GHGs composition can be used to identify the in-situ microbial metabolism within ice wedge ice (Lacelle et al., 2011b). The in-situ microbial activity can be also supported by significantly higher concentrations of CO_2 and CH_4 compared to mean atmospheric GHG compositions during the time when the ice wedges formed, whereas gas concentration also be altered via abiotic mechanisms such as melting – refreezing of the ice.

Previous studies have reported negative correlation between CO_2 and CH_4 mixing ratios in ice wedges, which may be attributed to *in situ* CH_4 oxidation in aerobic condition (Brouchkov and Fukuda, 2002) that can be inferred by carbon isotope fractionation factors (ε_C) between CO_2 and CH_4 (Whiticar, 1999). Moreover, study on the production and consumption of N_2O gas in the ice wedges have not been well reported except for the latest study of Kim et al. (2019). They identified the exclusive relation between CH_4 and N_2O N_2O (i.e., high (low) CH_4 only when N_2O is very low (high)), implying the influence of methanogenic activity and their inhibition by nitrogen compounds (Yang et al., 2023).

In contrast with CO_2 and CH_4, N_2O is produced (or consumed) by individual pathway related to the nitrogen cycle. Therefore, N_2O composition can be provide further information along with CO_2 and CH_4 in terms of more definite microbial activity within the ice wedge.

On the other hands, former studies on the origin of GHGs in ice wedges have mainly focused

only in terms of biological effect (Boereboom et al., 2013; Kim et al., 2019; Lacelle et al., 2011b), and the excess gas dissolution effect by liquid water has not been quantitatively investigated. Given that the different solubility in water for each GHGs, it is expected that the excess GHGs in ice wedges generated by the infiltration of liquid water can be determined.

Regarding gas analysis, Kim et al. (2019) utilized a developed analytical method which can simultaneously measure three GHGs (CO_2, CH_4 and N_2O) in one ice subsamples for precise comparison between GHGs composition. However, Ar-O_2-N_2 gas measurement and water chemistry analysis was separately performed. Thus, potential analytical bias cannot be ruled out completely due to sample inhomogeneity.

Although numerous ice wedge studies have been conducted up to the present, most of them have focused on samples near the seashore rather than inland (Opel et al., 2011; Streletskaya et al., 2015; Porter and Opel, 2020; Campbell-Heaton et al., 2021; Vasil'chuk et al., 2021). Comparing the features of these two regions, water chemistry of Siberian ice wedges near at the seashore was more likely to reflect the Pacific moisture than inland ice wedges, so that heavier isotope signature are prevailed in coastal ice wedge samples (Kurita et al., 2004).

Opel et al. (2019) clearly shows the “continental effect” of the interior Yakutian ice wedge from Siberia through water stable isotope data. The mean $\delta^{18}O$ values of inland Holocene ice wedge (213±109 ^{14}C yr BP) at the Adycha River (67.66°N, 135.69°E) was observed more depleted (mean values of −29.0 ‰) than other Holocene ice wedge sites in near the Northeastern Siberian Sea (mean values between −27.0 and -23.0 ‰), reflecting more continentality and relatively lower winter air temperature than the coastal sites (Opel et al., 2019). However, although research on inland ice wedges have been conducted, the number of the inland study is still insufficient. To compensate spatial bias due to unevenly distributed data and to better constrain spatial properties of diverse ice wedges, it is essential to supplement inland ice wedge data.

In this study, I analyzed ice wedge samples from Zyryanka, northeastern Siberia (Figure 1), and multiproxy study was carried out for multiple gas species, stable water isotope ratio of ice meltwater, and air bubble shape to better understand the formation mechanism of the ice wedge and origin of greenhouse gas species.

Compared to previous studies, this work takes an advantage of simultaneous analyses of three species of GHGs (CO_2, CH_4 and N_2O) and Ar-O_2-N_2 gas as well as the stable water isotopes for the same single ice wedge ice subsamples. This procedure can help avoid bias from inhomogeneous distribution of chemicals and consequently better constrain the ice wedge formation process. Moreover, we compare our ice wedge sample with modern precipitation in interpreting the δD- $\delta^{18}O$ relationship, which helps us constrain the season of the ice wedge formation and test the reliability of water isotopes as a winter paleoclimate proxy archive.

Chapter 2. Materials and Methods

2.1. Site description and ice wedge samples

Ice wedge samples were collected from the Zyryanka region in northeastern Siberia, Russia. Zyryanka is at 65°93′N, 150°89′E and located in the southern boreal region of the Kolyma River at the junction of the Chersky and Yukaghir Ranges (Figure 1), where is affected by thermokarst development (Fedorov et al., 1991). The region is underlain by the Holocene alluvial and the Pleistocene lacustrine-alluvial deposits with an average annual air temperature of -11.1℃ (Fedorov et al., 2014). Mean annual, January, and July air temperature for the last three decades at the Zyryanka meteorological station were -10.3, -36.2, and 16.2°C, respectively (Gidrometeoizdat, 1989). I used the samples from two Zyryanka sites (A and B), and ice wedge at site A were more intensively analyzed because the ice wedge at site A maintained a more symmetrical shape than at site B, so that the horizontal profile of geochemical properties was expected to indicate the same manner.

Ice wedge of Zyryanka site A with exposed width of about 2.0 m was selected for sampling (Figure 2). The top of the sampled ice wedge was about 1.7 m below ground surface, and block samples (W1-A to W1-H) were taken horizontally at the depth about 2.5 m from the ground. W1-B to F samples correspond to pure ice wedge, whereas W1-A, G and H samples are texture ice formed by refrozen soil water which consists of various natural waters (e.g., seasonal precipitation, surface waters, underground waters and so on).

A block sample was taken at a 2.0 m lower location from the upper block samples. Sediments adjacent to and over W1 consist of silt, peat, and numerous plant roots, peaty organic matter, and tree fragments.

Zyryanka site B was about 14 km west from entrance of a tributary of Kolyma, which starts from about 11 km north of Zyryanka. Top of sampled ice wedge started from about 1.2 m below

the ground surface. Width of the ice-wedge top was about 2 m. The site B ice wedge was surrounded by highly ice-rich sediments with gray silt, which contains chunks of peaty organic matter sometimes with larger tree trunks. Block samples were collected horizontally from upper (B_UpLeft-1 and B_UpLeft-2) and lower (B-Low-A to B-Low-D) potion of the ice-wedge exposure. Depths of the sampling lines from the ground surface were 2.5 and 3.1 m, respectively. A horizontal 15 cm thick sediment band with lenticular cryostructure intersected the ice wedge just above the lower sampling line.

2.2. Gas extraction method

The gas occluded in the ice wedge ice was extracted using a wet extraction method at Seoul National University (SNU). Wet extraction method has great advantage of minimizing gas loss and thoroughly extracting gas from ice subsamples. Fifteen and nine samples from the Zyryanka site A and B were selected for analysis respectively, and approximately 50 grams of each ice subsamples were cut and used for experiment. Each ice subsample was put in exclusive glass flask, allowing repeated artificial melting-refreezing processing in an ethanol bath maintaining the temperature at -75℃. The chemical/biological alteration in the original gas composition during the melting-refreezing process are negligible (Yang et al., 2020). The extracted gas was then cryogenically trapped in a stainless-steel sample tube at a temperature of -257℃. After which the stable water isotopes could be analyzed using the remaining ice meltwater after gas extraction. The more details about experimental processes for measurement are well described by Yang et al. (2020).

2.3. Radiocarbon dating

Radiocarbon age dating was carried out for the ice wedge and its adjacent texture ice through gaseous phase (^{14}C-CO_2) and plant debris enclosed in ice-wedge ice. Because the ice wedge at

Zyryanka A site is well developed in an ideal symmetrical wedge form, it could be inferred that the ages will also be assigned in the same manner depending on common ice wedge formation process (with younger center and older side part). For the radiocarbon age dating of Zyryanka A site ice wedge, identifiable enclosed plant debris (with a mean weight of ~2 mg) were sorted out at the adjacent soil on both side and gas was extracted in pure ice wedge where plant materials were insufficient. Pretreated plant remain samples were radiocarbon dated by an AMS at Beta Analytic Inc. and to constrain and compare with age from plant materials, CO_2 gas was also analyzed at the same company.

2.4. Greenhouse gas and Ar-O_2-N_2 mixing ratios

The measurement of GHG concentration was carried out at Seoul National University using a gas chromatograph (GC) system. For detection of the amount of CH_4 and N_2O in the extracted sample air, Agilent 7890B GC with a flame ionization detector (FID) and electron capture detector (ECD) was utilized. For CO_2 measurement, Agilent 7890A GC equipped with a FID was used. Furthermore, I measured the Ar-O_2-N_2 concentration of gases extracted from a single ice subsample using the methods mentioned above. Agilent 7890B GC with a thermal conductivity detector (TCD) was utilized for the Ar-O_2-N_2 gas analysis. The $\delta(N_2/Ar)$ and $\delta(O_2/Ar)$ value are expressed in percent (%), compared to the reference from the present-day molar atmospheric ratio, and are represented by the following equation:

$$\delta(X/Ar) = \left(\frac{\left(\frac{X}{Ar}\right)_{sample}}{\left(\frac{X}{Ar}\right)_{air}} - 1 \right) \text{ X } 100\ (\%) \qquad \text{(Equation 1)}$$

where X = N_2 or O_2. Ar, O_2 and N_2 composition in the atmosphere has consistently maintained during the Quaternary (Holland et al., 1984). Therefore, $\delta(N_2/Ar)$ and $\delta(O_2/Ar)$ carry implication of gas alteration during or after ice-wedge formation.

2.5. Stable water isotopes

Stable water isotope ratios were analyzed for fifteen and nine subsamples from Zyryanka A and B site ice wedge, respectively with the horizontal intervals of 8-cm in outcrop. In addition to that, the same analysis was also conducted for the modern precipitation in the Zyryanka region.

Stable water isotope compositions ($\delta^{18}O$ and δD) for ice meltwater remaining after the gas extraction from the ice-wedge ice and modern precipitation were expressed in per mil (‰) relative to the Standard Mean Ocean Water (SMOW) as follows:

$\delta_{sample} = \left(\frac{R_{sample}}{R_{SMOW}}\right) X 1000$ (‰), where R is $^{18}O/^{16}O$ or $^{2}H/^{1}H$ (Craig, 1961).

Furthermore, deuterium excess (d-excess = $\delta D - 8 \times \delta^{18}O$) was calculated for clarifying moisture source change and ice wedge formation process.

Water isotope compositions of ice wedge and some precipitation samples were analyzed at Ewha Womans University, Korea using an L2140-i model isotopic water liquid analyzer (Picarro Inc., Sunnyvale, CA, USA), via Wavelength-Scanned Cavity Ring-Down Spectroscopy (WS-CRDS) method. Each ice meltwater sample was filtered out organic matter and any impurities using a 0.45-μm syringe filter. The internal standards were USGS 46, 47, and 48 with 1σ of less than 0.1 ‰ for $\delta^{18}O$ and less than 1 ‰ for δD, respectively. Moreover, water chemistry analysis for additional precipitation samples was carried out at the Isotope Hydrology Laboratory of Kumamoto University, Japan using a cavity ring-down spectroscopy isotopic water analyzer (L2120-I, Picarro Inc., Sunnyvale, CA, USA) with analytical errors are 0.2 ‰ and 0.6 ‰ for $\delta^{18}O$ and δD, respectively. More detailed analytical procedure was described well in Ichiyanagi et al. (2019) and Laonamsai (2021).

2.6. Carbon isotopes

The target gas extraction and collection procedures for analysis of $\delta^{13}C$-CO_2 and $\delta^{13}C$-CH_4 are identical to those described in section 2.2. The gas samplers were sent to Nagoya University in Japan for determining carbon isotope ratio of both target gases. The continuous flow isotope ratio mass spectrometry (CF-IRMS) system was applied for determining $\delta^{13}C$ of CO_2 and CH_4, and the more details about experimental and analytical protocols are well elucidated in Kawagucci et al (2005) for CO_2 and Hirota et al (2010) for CH_4, respectively.

To better understand the origin of CO_2 gas in ice wedge, I also measured the carbon isotope signatures of various substances in the surrounding ice wedge environment along with the ice wedge. $\delta^{13}C$ analysis for plant remains in ice wedge and for dissolved inorganic carbon (DIC) using the about 8 ml of ice wedge meltwater were carried out via an isotope ratio mass spectrometer (IRMS) at Beta Analytic Inc. For both soils trapped in and adjacent to the ice wedge, carbon isotope signatures were determined using an isotope ratio mass spectrometer (IRMS) at the National Instrumentation Center for Environmental Management (NICEM) at Seoul National University, Korea. All the carbon isotope ratios are expressed relative to standards of Vienna Pee Dee Belemnite (VPDB).

Chapter 3. Results

3.1. Radiocarbon dating

The mean radiocarbon age of Zyryanka ice wedge and the texture ice adjacent to ice wedge was measured at 810 to 1750 years before present (yrs BP, present = 1950 CE), (*n*=3) and 3900 to 4430 yrs BP (*n*=8), respectively (Table 1), inferring that this ice wedge and adjacent soil were formed during the late Holocene. For the adjacent soils, comparing the CO_2 gas ages of 4090 ± 63 yrs BP, the ages of plant debris (4300 ± 40 yrs BP) agree well with those of CO_2 gas although the average CO_2 gas age was slightly younger. Figure 5 shows the age distribution of Zyryanka A site ice wedge by position. It should be noticed that the horizontal error bar indicates the length of the subsample, not the measurement errors. Ice samples with a distance of 80-175 cm from the left end were used for the CO_2 gas age dating for pure ice wedge. The error for each measurement age (vertical error) is 30 years, but the vertical axis is very wide at 1000 years intervals, showing no vertical errors in the figure.

If part of CO_2 composition had been formed by the reaction of carbonate minerals with acids, the CO_2 age would have been much older than the age of plant remains. However, I can rule out the possibility that CO_2 was formed by the reaction of carbonate minerals because CO_2 age is actually observed to be similar to or slightly younger than the age of plant remains.

3.2. Ar-O_2-N_2 mixing ratios

3.2.1. $\delta(N_2/Ar)$ and $\delta(O_2/Ar)$

Ar, O_2 and N_2 gas mixing ratio of the occluded gas reflect the origin of infilling material of the ice wedges and the existence of microbial respiration within ice-wedge ice (St-Jean et al., 2011; Lacelle et al., 2011b). The formation process of ice wedge can be understood using N_2/Ar

molar ratio or noble gas ratio. Since N_2 and noble gas are soluble gases in water with little effect on the biological activity, they can determine whether ice wedges have experienced melting under open air. Accordingly, if ice wedge experienced annual thawing-refreezing, the gas compositions in the ice can be altered compared to atmospheric gas ratio. If the ice wedge is formed exclusively by freezing liquid water, $\delta(N_2/Ar)$ and $\delta(O_2/Ar)$ value is close to -55.5% and -8.97%, respectively, assuming the atmospheric gas is equilibrated with 0℃ of water. On the other hand, if ice wedge was formed by either dry snow accretion or hoarfrost growing rather than meltwater freezing, both $\delta(N_2/Ar)$ and $\delta(O_2/Ar)$ should be close to the atmospheric value of 0 %. $\delta(N_2/Ar)$ value of Zyryanka A site ice wedge ranges -17.5 ~ -3.5%, which is less than zero in all samples (Table 2, Figure 3). $\delta(O_2/Ar)$ values of ice wedge exhibit a range from -72.8 to -37.58 %, implying that O_2 has partially been consumed. For the values of soils adjacent to ice wedge, $\delta(N_2/Ar)$ values range from -43.9 to -1.8 % and $\delta(O_2/Ar)$ shows a lower value range of -99.1 to -83.1%.

3.2.2. Fraction of gas originated from dissolved gas in liquid water

I applied the $\delta(N_2/Ar)$ ratio to estimate the fraction of gas originated from dissolved gas in liquid water (i.e., snow meltwater), and defined this parameter as “liquid water fraction(f)” hereinafter. The mole fraction of N_2 and Ar in the atmosphere is different from that of 0°C water, providing standard molar ratio of 83.60 for N_2/Ar. Therefore, assuming that equilibrium state after the gas exchange between potential liquid water and atmospheric air, I can derive the equation for mixing ratio of the measured gas as follows (where “mix” refers to admixture of gases which are originated from liquid water and atmospheric air):

$$\left(\frac{N_2}{Ar}\right)_{mix} = \frac{0.78(1-f) + 0.63f}{0.00934(1-f) + 0.0170f} \qquad \text{(Equation 2)}$$

Where, f= liquid water fraction.

Based on this, $\delta(N_2/Ar)_{mix}$ can be calculated as follows:

$$\delta(N_2/Ar)_{mix} = \left(\frac{\left(\frac{N_2}{Ar}\right)_{mix}}{83.60} - 1\right) \text{x } 100\ (\%) \qquad \text{(Equation 3)}$$

Therefore, following equation for liquid water fraction can be deduced:

$$f = \frac{-0.78 * \delta\left(\frac{N2}{Ar}\right)_{mix}}{64.805 * \left(\frac{\delta\left(\frac{N2}{Ar}\right)_{mix}}{100} + 1\right) + 15} \qquad \text{(Equation 4)}$$

Using this liquid water fraction value, the gas dissolution effect can be corrected in the gas composition.

3.3 Greenhouse gas compositions

I observed that three greenhouse gas compositions (CO_2, CH_4, N_2O) of the trapped gas within the ice wedge were significantly higher than that of the Holocene atmospheric level. Given that the average greenhouse gas composition during the late Holocene (Rubino et al., 2019) at the ages of Zyryanka ice wedge, our observed data are measured approximately two or three order of magnitude higher than the atmospheric value (Table 2). Furthermore, I also observe that the gas concentration is relatively higher in the adjacent soils than in the pure ice wedge part (Figure 4) and the soil amount and liquid water fraction shows in the same manner.

3.4. Stable water isotope distribution

Stable water isotope values obtained from ice meltwater of ice wedge can afford further information concerning formation processes of ice wedge. The mean $\delta^{18}O$ value of the ice wedges in the Zyryanka A and B site are -28.14 ‰ and -28.79 ‰, and mean δD values were

measured as -218.9 and -223.5 ‰, respectively (Figure 5, Table 2). The mean value of deuterium excess(d-excess) of the Zyryanka ice wedge is 6.21‰. It is observed that relatively lower $\delta^{18}O$ values of -28.14 ‰ in the ice wedge part, whereas higher values of -21.85 ‰ are shown at which is adjacent soil part of the ice wedge. The $\delta^{18}O$ and d-excess trend is characterized by distinct symmetric structure with respect to the center part in both Zyryanka A and B site ice wedges (Figure 5). Moreover, I gained local meteoric water line (LMWL, $\delta D = 7.46 * \delta^{18}O - 9.24$) through $\delta^{18}O$ and δD values of monthly precipitation in September 2017 to May 2020 (*n*=189) at Zyryanka region. LMWL determined within the Zyryanka region is nearly consistent with regression of Siberian Network of Isotopes in Precipitation (SNIP) stations ($\delta D = 7.93 * \delta^{18}O + 2.87$; Kurita et al., 2004), though the y-intercept is lower than SNIP.

3.5. Bubble shapes

Since the bubble formation process in wedge ice and its shape are closely related, the occluded air bubbles within the ice wedge ice were investigated to understand the ice wedge formation process more clearly. I observed that the bubble shape of different part of the ice wedge ice varies depending on the liquid water fraction of ice wedge (Figure 6 and 7). In section of ice wedge with relatively high liquid water fraction the bubble shape is elongated and has preferred specific orientation, whereas spherical bubbles were observed in parts where liquid water fraction is relatively small.

3.6. $\delta^{13}C$ of CO_2, CH_4, DIC, soil and plant remain

The mean $\delta^{13}C$ values of CO_2 and CH_4 from the Zyryanka A site ice wedge were -19.5 ± 1.2‰ (*n*=5) and -69.5 ± 0.5 ‰ (*n*=3) (Table A5), respectively. In contrast with our initial expectation that the $\delta^{13}C$-CO_2 would reflect typical C_3- derived organic matter with $\delta^{13}C$ = -27‰ (Ehleringer et al., 2000), obtained results show more enriched value of about 7.5‰. For these

results, it can be implied that the partial CO_2 was likely produced through materials other than organic carbon. On the other hand, the $\delta^{13}C$ value of CH_4 of -69.5 ‰ agrees well with the value attributed in bacterial origin, rather than thermogenic origin, based on the reported ranges of -110 to -50 ‰ for bacterial origins (Whiticar, 1999).

For the carbon isotope signatures of soils and plant remains in both Zyryanka A and B site ice wedge, they reflect typical C_3- type material (Staddon, 2004) with the mean values of -26.6 ‰ (Table A6 and Figure 11), regardless of their origins (ice wedge or adjacent soils).

On the other hand, the mean $\delta^{13}C$ value of DIC for the ice wedge and adjacent soils from the Zyryanka A site were -13.1 and -16.8 ‰, respectively, and those from the Zyryanka B site were -7.96 and -8.3 ‰, respectively, showing more enriched carbon isotope values at the Zyryanka B site than the A site.

Chapter 4. Discussion

4.1. Formation of ice wedge

The ages of the ice wedge part of Zyryanka A site (Zy-A-W1-B to F) covers from 810 to 1750 years before present (BP, present = 1950 CE), whereas adjacent soil part (Zy-A-W1-A and W1-G to H) covers from 3900 to 4430 years BP. Based on the significant age gap between the ice wedge and adjacent texture ice, it can be estimated that the ice wedges began to develop at least 2700 years after the adjacent soil was deposited. The age at Zyryanka B site ice wedge was analyzed only for upper ice block samples (B-upleft2) using plant residue, showing 4830 ± 30 years BP. Because the plant residue inside the ice wedge comes from the neighboring soils and the measured age corresponds almost to the adjacent soil age of A site, it can be inferred that the sediments of the site B was also formed at the similar time as the site A.

Mackay et al (1972) found that normal size ice wedge (about 1-2 m) can be preserved a higher temporal resolution because the cracking probability is much higher than that of relatively wide ice wedges, so that they are more likely to show ideally gradual age variation. Zyryanka ice wedge (with 2.0 m width) fit in this case, so that younger center-older side pattern can be observed from a horizontal age distribution of the ice wedge profile.

Comparing to the last glacial period (LGP) ice wedges in Yakutsk area (e.g., Kim et al., 2019) whose $\delta(N_2/Ar)$ value is generally close to, even greater than zero, the Holocene Zyryanka ice wedge shows significantly low $\delta(N_2/Ar)$ values (Figure 3), indicating that it was formed by partial melting of ice or by mixing of liquid water with snow, rather than only hoarfrost compaction. To confirm the influence of liquid water, I examined bubble shapes in ice-wedge ice. If an ice wedge has once experienced melting-refreezing process or infiltration of liquid water, the occluded bubble likely shows elongated cylindrical shape (Boereboom et al., 2012). Meanwhile, the bubble shapes are almost spherical when the ice created with dry snow

compaction or hoarfrost accretion (St-Jean et al., 2011). For that reason, the presence of elongated bubbles in some parts of the Zyryanka ice wedge ice indicates that it may have been experienced partial melting or infiltration of liquid water. If that is the case, it becomes important to constrain the exact point in time when liquid water formed. In fact, it is more reasonable to that some liquid water was pre-formed at the active layer and permeated into the ice wedge cracks during the ice wedge formation, rather than the *in situ* liquid water production in ice wedge (which can be caused by melting or compaction of ice). With respect to this will be discussed in detail afterward.

Regarding to the regional characteristics of ice wedges, comparing the mean $\delta^{18}O$ values of Holocene ice wedges at near the northeastern Siberian Sea coast (-25‰; Meyer et al., 2002a; Wetterich et al., 2008; Meyer et al., 2015; Streletskaya et al., 2015; Opel et al., 2017), values of inland Zyryanka ice wedge generally much lighter than that (-28.6 ~ -27.4‰) due to the "continental effect" derived from depletion of heavy isotopes in inland areas compared to regions closer to the Pacific vapor sources (Kurita et al., 2004; Strauss, 2010). In this respect, I should note that stable water isotope composition of ice wedges reflects regionality as well as the air temperature of a given region.

Previous studies have questioned whether the ice wedge can be used as paleoclimate proxy because isotopic diffusion can modify the isotope signature of ice (Meyer et al., 2007; Meyer et al., 2010a; Opel et al., 2011). For the Zyryanka ice wedge case, $\delta^{18}O$ distribution shows the symmetrical enrichment in heavy isotopes towards the edge of the ice wedge body (Figure 5).

It can be estimated that liquid from adjacent soils on both side parts did not affect to the water isotope chemistry of ice wedge, given the following various evidences that: (1) significantly different $\delta^{18}O$ values between the ice wedge and the adjacent texture ice (-28.14 ± 0.4 and -21.85 ± 2.0 ‰, respectively), (2) sharply increased $\delta^{18}O$ value profile from the ice wedge to adjacent texture ice, and (3) small variation of the $\delta^{18}O$ values of the ice wedge (with a mean

of -28.14‰, SD=0.39). However, we cannot fully rule out the effect of liquid water originated from upper active layer on ice wedge formation because the central crack in ice wedges extending to the ground surface allows water in contact with the atmosphere and/or in the active layer soil to infiltrate sufficiently into the ice wedge.

On the other hand, it can be simply inferred that summer precipitation (from May to September) did not considerably attribute to the ice wedge formation given the assumption that ice wedges are mainly fed by winter precipitation (Vaikmäe., 1990), so that the material charging ice wedge cracks dominantly preserves a winter climate signal. Furthermore, minor snowfall amounts of summer periods (from May to September; about 12% of total snowfall) with significantly heavier $\delta^{18}O$ values compared to that of ice wedge (mean value of -21 and -28 ‰ for summer precipitation and ice wedge, respectively) are also elucidate major contribution of winter precipitation for Zyryanka ice wedge formation. The average snowfall and mean air temperature of Zyryanka region along with $\delta^{18}O$ values of Zyryanka precipitation and ice wedge are shown in figure 9.

In this regard, interesting point is that contribution of liquid water to the Zyryanka ice wedge formation was clearly identified, given the negative $\delta(N_2/Ar)$ values of ice wedge.

According to Beria et al (2018), the oxygen and hydrogen isotope compositions ($\delta^{18}O$ and δD) of snow vary along the meteoric water line (MWL) during an equilibrium process (e.g., condensation), while the isotope values of $\delta^{18}O$ and δD must deviate from the MWL during a non-equilibrium process (e.g., evaporation and sublimation). In the ice wedge and precipitation co-isotope relationship ($\delta^{18}O$- δD) diagram, it can be observed that the regression slope and y-intercept for Zyryanka ice wedge ($\delta D = 7.24* \delta^{18}O – 15.2$) are almost identical to our modern local meteoric water line (LMWL) of Zyryanka region ($\delta D = 7.46* \delta^{18}O – 9.2$) (Figure 8). According to Opel et al (2011), the coincidence of the water isotope chemistry of the ice wedge and the GMWL in the $\delta^{18}O$-δD diagrams imply that minor influence of kinetic fractionation

processes. Because our LMWL is nearly consistent with that of Siberian Network of Isotopes in Precipitation (SNIP) station ($\delta D = 7.93 * \delta^{18}O + 2.87$; Kurita et al., 2004) as well as with GMWL ($\delta D = 8 * \delta^{18}O + 10$), it can be accordingly inferred that this ice wedge was formed in equilibrium condition without any noticeable secondary isotopic fractionation that can be caused by evaporation or snow sublimation. On the other hand, Boike (1998) and Meyer et al (2002a) suggested that any potential physical alteration processes of ice wedges caused by *in situ* evaporation, sublimation and snow meltwater percolation can cause a significant modification of d-excess in the snow. Furthermore, d-excess of precipitation is used to verify any changes in the moisture source condition and switches of precipitation sources (Jouzel, 2003). In the Zyryanka ice wedge case, the mean d-excess value of the ice wedge of 6.21 ± 0.73 ‰ is very similar to the local modern winter precipitation value of 5.86 ± 5.14 ‰ (mean ± σ, which is average for October to April). Given this result, it can be inferred that modification of isotopic composition of winter precipitation feeding the ice wedge was negligible, and that the moisture source conditions have not changed significantly from the ice wedge formation period (1.3 ka, which is correspond to the late Holocene) to the present day.

According to the established theory that the mean annual air temperature at mid- and high latitudes is highly correlated with mean stable water isotope value of annual precipitation (Dansgaard, 1964), and the more progressed study about paleotemperature reconstruction equation for winter by Vasil'chuk (1993; $T_{mean\ winter} = \delta^{18}O_{ice\ vein}$ (± 2°C) and $T_{mean\ January} = 1.5 * \delta^{18}O_{ice\ vein}$, where T=air temperature), the water isotope composition of the recent ice wedge vein should be approximately identical to the winter air temperature at that time.

In this context, assuming that: (1) the water isotope chemistry of precipitation in a given study site has not changed significantly from the late Holocene to the present, and that (2) the original isotope composition of winter precipitation trapped in the ice wedge has been well preserved without any isotopic alteration, it may be possible to compare the water isotope composition

between the late Holocene ice wedges and modern precipitation.

In this regard, I compared $\delta^{18}O$ composition of the Zyryanka ice wedge with modern winter air temperature in Zyryanka region depending on each arbitrarily set winter period, and it was confirmed that the difference between the two values is not constant (Table A7). This result indicates that it may not be appropriate to apply the Vasil'chuk's equation as it is for reconstruction of paleotemperature unless the winter period is clearly constrained.

On the other hand, according to the established theory that ice wedges are mainly formed by filling winter precipitation (Vaikmäe., 1990), water isotope chemistry of ice wedge should reflect the composition of winter precipitation as it is. I observed that mean precipitation-weighted $\delta^{18}O$ signature of given arbitrary winter period is higher 3 ‰ on average than that of Zyryanka ice wedge, except for the period of October to April. Therefore, more obvious basis is needed to explain why the $\delta^{18}O$ value of the Zyryanka ice wedge is relatively enriched than almost winter precipitation value.

Accordingly, following two hypotheses can be suggested to clarify 3‰ deviation between $\delta^{18}O$ signature of winter precipitation and ice wedge. First, winter period in Zyryanka region can be defined as period from October to April. Winter period varies by region and several studies investigating the water isotope chemistry of modern seasonal precipitation in circumpolar regions have generally defined winter as the period when precipitation falls as snow (Nikolayev and Mikhalev, 1995; Streletskaya et al., 2015; Meyer et al., 2010a; Meyer et al., 2015; Meyer et al., 2022). In fact, the modern air temperature in Zyryanka remains below 0°C from October to April (hereafter referred to as ice-wedge winter, Pogodaiklimat Nov 03, 2022, Figure 9), and precipitation type during this period is snow, so that I can undoubtedly define this period as winter. Accordingly, because the $\delta^{18}O$ value of winter precipitation of Oct.- Apr. (-28.40 ‰) almost identical to the Zyryanka ice wedge value (-28.46 ‰), it can be inferred that the precipitation during this period mainly contributed to the formation of ice wedge.

Furthermore, it can be possible to constrain our own paleotemperature reconstruction equation for the Zyryanka region. Dansgaard's (1964) empirical δD_{precip}-air temperature relation (δD_{precip}= 5.6 ‰· °C^{-1} × temperature (°C) - 100‰; Dansgaard, 1964) has commonly used to estimate Mean Annual Temperature (MAT) in mid-to high latitude. However, our own equation was determined as δD_{precip}= (2.61 ± 0.3) ‰· °C^{-1} × T_w (°C) – (169.54 ± 6.7) ‰ (R^2 = 0.37, *n*=149, where T_w= ice-wedge winter temperature), which slope coefficient is roughly half as steep as that of Dansgaard (1964). This indicates that appropriate calibration of regional and monthly biases is mandatory (Rozanski et al., 1993). Data used for establishing our new equation reflects the average values of each monthly precipitation corresponding to Oct. to Apr. in 2017-2020.

Interestingly, however, a study about Late Holocene paleotemperature reconstruction for Northwestern Canada region, also reported δD_{precip} – winter temperature relation (δD_{precip}= (3.1 ± 0.1) ‰· °C^{-1} × temperature (°C) – (155 ± 1) ‰; Porter et al., 2016), which is almost identical to our result. Referred study also observed good agreement between the δD_{precip} from Oct to May obtained at local GNIP station and δD value of Late Holocene ice wedge, as well as between the measured surface air temperature from Oct to May and theoretical temperature calculated by δD_{precip}-T equation (Porter et al., 2016). Likewise, similar temperature-isotope relation coefficients were also determined in northeastern Siberia, showing δD_{precip}-T equation of δD_{precip}= 3.1 ‰· °C^{-1} × temperature (°C) – 143.7 ‰ (defined as winter from November to April; Wilkie et al., 2012). In this context, our slope coefficient and y-intercept show good agreement with previously reported results, so that this is universally derived results and our new δD -T equation can be appropriately used in our study region.

Meanwhile, our new δD –T_w equation can be rearranged for ice-wedge winter temperature (T_w) as follows:

T_w= (0.1421 ± 0.01) °C · ‰$^{-1}$ × δD (‰) + (10.794 ± 3.5) °C, R^2 = 0.3709 (Equation 5)

Using Equation 5, the theoretical T_w estimated based on the Zyryanka ice wedge δD (-218.92‰) are calculated to be -19.9 ± 3.5 °C, indicating the expected Oct-Apr air temperature at the time when the Zyryanka ice wedge formed. It should be noted that the ice wedges are formed by composite of all precipitation during the ice wedge growing period, leading to a blended sample that is weighted by snowfall amounts of each precipitation event. In other words, ice wedge δD is isotopically weighted by contribution of precipitation during periods when snowfall amounts are relatively high. Thus, the induced theoretical T_w is also a precipitation-weighted value, where I assume that the monthly snowfall during the ice wedge growing period is identical to the present. Accordingly, compared to the precipitation-weighted modern Oct-Apr air temperature (-22.7 °C), it can be inferred that the induced theoretical T_w is reasonable considering the error in terms of reconstruction of paleotemperature in the Late Holocene.

However, the estimation error (±3.5°C) of the theoretical temperature is too large to constrain the climate variability during the Holocene. Future studies should fully consider the validity of this error.

However, if the Zyryanka ice wedge was not formed by precipitation in October-April, the possibility of isotopic alteration by other impurities still remains, given the difference of 3 ‰ $\delta^{18}O$ between the precipitation-weighted value for other arbitrary winter period and the ice wedge except for period of October to April. As another cause of this difference therefore, soil pore water may have infiltrated and modified the original isotope signature of ice wedge. With regard to the soil environment of the Zyryanka ice wedge, a thick silt and clay layers are located above the peat soil layer surrounding the ice wedge. In fact, it was clearly observed that the soil types in the ice wedge are silt and clay, so that it is likely that pore water originated from the uppermost active layer soil penetrated the ice wedge with the soil along the center crack of the ice wedge. Accordingly, increased ice wedge δD values is likely due to the contribution of relatively enriched δD value of pore water included in soils adjacent to the ice wedge (*ca.* -

179.3 ‰). In conclusion, it should be considered the effect of surrounding impurities that can sufficiently modify the original chemistry of ice wedge, which cause uncertainty of ice wedge as a paleoclimate proxy. However, because no significant isotopic alteration by neighboring soils was observed in Zyryanka ice wedge, it can be ruled out the effects of soils, implying that paleoclimate signature of Zyryanka ice wedge remain well-preserved, so that this ice wedge can play an important role as a paleoclimate proxy.

4.2. Origins of gases within ice wedge ice

4.2.1. O_2

$\delta(O_2/Ar)$ values exhibit a wide range from -72.9 to -37.6 %, which may imply that O_2 has been consumed somewhat (Table 2, Figure 3). In figure 3, interestingly, $\delta(O_2/Ar)$ values of Zyryanka ice wedge seems to be admixture between adjacent soil and atmospheric ratio end-members in a plot of $\delta(O_2/Ar)$ versus $\delta(N_2/Ar)$ ratio. I already identified no significant effect of gas diffusion from adjacent soils to ice wedge, whereas the possibility still remains that liquid materials contacted with the active layer soils above the ice wedge penetrate the opened ice wedge cracks. Assuming that the snow mass in contact with the atmosphere produce liquid water at the interface of active layer soil - snow mass, composition of active layer soil is similar to that of soils adjacent to the ice wedge on both sides, and gas equilibrium with atmosphere is maintained, ice wedge can fully reflect oxygen gas compositions of soil and atmosphere.

In here consequently, I can suggest two possible hypotheses for the negative $\delta(O_2/Ar)$ values of Zyryanka ice wedge; (1) selective consumption of oxygen by *in situ* microbial respiration and (2) admixture of oxygen composition of soil and atmosphere.

4.2.2. CO_2

Compared with previous study about greenhouse gas composition in last glacial period (LGP) ice wedges at Central Yakutia (Kim et al., 2019; Yang et al., 2023), CO_2 mixing ratio (*ca.* 3.1%) in Zyryanka ice wedge is observed to be about a third of the LGP ice wedge values (*ca.* 9.6%, Kim et al., 2019; Yang et al., 2023).

For the carbon isotope composition of CO_2 gas, I initially expected that the stable carbon isotope value of CO_2 ($\delta^{13}C$-CO_2) for Zyryanka ice wedge would reflect typical C_{3}- derived organic matter with $\delta^{13}C$ = -27‰ depending on the high CO_2 compositions of *ca.* 30900 ppm. However, average $\delta^{13}C$-CO_2 signature of -19.5 ‰ (n=5) for ice wedge imply that the excess CO_2 was likely produced by other source materials. For this reason, the potential influence of anthropogenic CO_2 such as coal combustion fumes can be expected. Although there is a coal mine located about 20km south of the research area, it is difficult to say that it affected to the gas composition of Zyryanka ice wedge formed in late Holocene because the development of coal mining did not take place until the 20th century.

This relatively enriched carbon isotope signal of CO_2 can be derived from various processes: (1) mixing with atmospheric air, (2) carbonate weathering, (3) CO_2 originated from C_{4}- plant, and/or (4) dissolved inorganic carbon (DIC). First, mixing with atmospheric CO_2 will enrich the $\delta^{13}C$-CO_2, since the $\delta^{13}C$ value of CO_2 of atmospheric air is approximately -6.5‰ (Bauska et al., 2015) in the Late Holocene period. Moreover, observed CO_2 composition is too great to be considered atmospheric air mixing as a main cause of isotopic alteration with regard to the Holocene mean atmospheric CO_2 level of 280 ppm (Rubino et al., 2019).

With regards to contribution of geogenic DIC, ^{13}C-enriched signature is mostly represented the weathering of carbonate, which documented range is reported in the Coplen et al. (2002).

To substantiate the second assumption, carbon isotope analysis for soils occluded in ice wedge

was carried out to verify the presence of any carbonate contained minerals (e.g., calcite, dolomite, and rarely siderite) with typical $\delta^{13}C$ value of 0 ‰ (Land., 1980). Consequentially, difference of $\delta^{13}C$ signatures between natural and acid-treated soil samples (given as -28.5 and -28.4 ‰, respectively) shows insignificant, indicating that the ice wedge soil contains negligible carbonate minerals and the influence of that minerals on isotope signatures can be considered minor. However, influence of carbonate minerals on carbon compositions of ice wedge cannot be fully excluded in terms of dissolution to liquid water. Dissolution of the carbonate possibly take place if carbonate minerals included in the soil come into contact with water. In this case therefore, the possibility cannot be fully ruled out that existing soil carbonate minerals have completely been dissolved in water, so that their effects have not been observed at $\delta^{13}C$ value of soil. A more detailed description for modification in carbon composition by dissolved carbon will be described below.

On the other hand, plants preferentially take in the lighter $^{12}CO_2$, thus carbon in plants is depleted in ^{13}C compared to the atmosphere. Moreover, the fractionation is different in C_{3}- and C_{4}- plants: The $\delta^{13}C$ values ranges from -24 to -35 ‰ with a mean of -26 ‰ for C_{3}- plant whereas the C_{4}- plant has more enriched $\delta^{13}C$ values from -10 to -14 ‰ with a mean of -13 ‰ (Cerling et al., 1993; Cerling et al., 1997). Although CAM plant has a similar range of $\delta^{13}C$ values to the C_{4}- plant, that plant can exclusively survive at tropical or dry habitats (Lüttge, 2010), so that it can be supposed that they had minor contribution to the CO_2 composition of Zyryanka ice wedge. On the other hand, while C_{4}- plant also prefer the relatively warm- to high-temperature environments, it has been reported some species that can endure the cold temperature such as *Miscanthus* genus whose habitat is from northeastern Siberia (Raghavendra et al., 2011). Although $\delta^{13}C$-soil adjacent to Zyryanka ice wedge show average -28.4 ‰, $\delta^{13}C$-CO_2 for the respiration of plants grown in that soils need not be identical

(Ehleringer et al., 2000). For example, it causes a large $\delta^{13}C$ differences between soil CO_2 and soil organic matter when C_4- crop such as corn ($\delta^{13}C$ -11.8‰) grows in C_3- soils ($\delta^{13}C$ -25.7‰) (Rochette and Flanagan, 1997), resulting in $\delta^{13}C$-CO_2 more enriched than that of C_3- derived organic matter (Ehleringer et al., 2000).

In conclusion, although pollen studies have not been conducted in our samples, it cannot be ruled out the possibility that C_4- plant species was incorporated into the ice wedge with C_3- plants, leading to relatively enriched carbon isotope value of CO_2.

The paramount point I need to focus on is that Zyryanka ice wedge was formed by mixing of liquid water. Based on this observation, I therefore speculate that DIC- derived CO_2 gas may have contributed in part to the entire CO_2 composition. However, the measured CO_2 composition is too great to be described as simply due to gas dissolution in liquid water, so that the production by microbial respiration should be mainly considered. As already mentioned in Section 4.1., I deduced that the origin of liquid water that caused $\delta(N_2/Ar)$ ratio more depleted was in contact with active layer soil located above the ice wedges. Therefore, if that water permeates into the ice wedge through the cracks, it is likely that the DIC-derived CO_2 gas was also originated from that source water. That is, it is possible that CO_2 produced by microbial activity in the active layer soil was dissolved in liquid water infiltrating into the ice wedge cracks, and its chemical properties were reflected in the ice wedge. These hypotheses are sufficient to elucidate our measurement results.

According to Whiticar (1999), typical methanogenic pathway can be determined by considering relationship between $\delta^{13}C$-CO_2 and $\delta^{13}C$-CH_4 as well as formation water which can be pore water or any water mass. In terms of this relationship, carbon isotope fractionation factor (described in ε_C) can be calculated for combination of $\delta^{13}C$-CO_2 and $\delta^{13}C$-CH_4, associated with methanogenesis in freshwater environment (Whiticar, 1999).

ε_C values of CO_2-CH_4 for Zyryanka ice wedge was calculated as 49.8 ± 2 (mean ± 1σ), implying that methanogenesis was dominated by methyl-type fermentation (which ε_C values typically ranging from 40 to 55). That is, this result indicates that formation of Zyryanka ice wedge partially took place in freshwater condition. This result along with observed negative $\delta(N_2/Ar)$ values can support our theory that unfrozen water contributed to ice wedge formation, as well as that dissolved inorganic carbon is likely to influence carbon composition in ice wedge. That is, our enriched carbon isotope signal was possibly attributed to dissolved organic carbon (DIC).

$\delta^{13}C$ of DIC in soil generally reflect a mixing of three end-members, carbonate mineral dissolution, atmospheric CO_2, and soil CO_2 (Doctor et al., 2008; Campeau et al., 2017). Carbonate mineral dissolution generally occurs by reaction with carbonic acid, whereby DIC in solution (as HCO_3^-) is derived from the $CaCO_3$ and soil CO_2 (Doctor et al., 2008).

Dean et al (2020) reported carbon isotope compositions of various inland water sources, presenting that the value of DIC is much heavier (-22.9 ~ -12.1‰ $\delta^{13}C$) than that of particulate organic matter (POC, -33.7 ~ -30.6‰ $\delta^{13}C$, which is typical value of plant remains) or dissolved organic matter (DOC, -29.9 ~ -26.2‰ $\delta^{13}C$, with respect to freshwater DOC derived from C_3-plant photosynthesis). In fact, our measured $\delta^{13}C$-DIC data for Zyryanka ice wedge meltwater are included in the range of typical $\delta^{13}C$ value range for inland water DIC mentioned above, showing -13.1 ± 1.3 ‰ (mean ± 1σ), which can also be compared well to values presented from other Arctic watershed study ($\delta^{13}C$ -20 ~ -8 ‰; Throckmorton et al., 2015). Across the fluvial network, Drake et al. (2018) reported that ambient $\delta^{13}C$-DIC (-13 ~ -8 ‰) are more enriched relative to respiratory $\delta^{13}C$-DIC (-26 ~ -17 ‰), suggesting that pore water or meteoric water DIC was more contributed, or it constantly fractionated from the depleted product by soil respiration. In our case, average $\delta^{13}C$-DIC value from Zyryanka ice wedge was measured at -

13.1‰ (*n*=4), which is in good agreement with the reported ambient δ^{13}C-DIC value.

In general, outgassing of CO_2 in water will take place when partial pressure of CO_2 in solution is greater than that of the atmospheric air. According to Zhang et al. (1995), calculated isotope fractionation between aqueous and gaseous CO_2 ($\varepsilon_{aq\text{-}g}$) at 0°C shows -1.31 ‰, indicating only a small fractionation effect during converting dissolved CO_2 into gas CO_2.

Another possible elucidation of increased ice wedge δ^{13}C signature is soil carbon mixing; CO_2 remaining in the soil atmosphere (which is referred to as soil CO_2 hereafter) of the active layer can be incorporated into the ice wedge when the ice wedge cracks splits and the soil from the active layer is infiltrated in the ice wedge along the crack. Generally, soil atmospheric composition is more enriched of ^{13}C than the ^{13}C content of the decomposed organic matter (Cerling et al., 1991). Indeed, soil CO_2 is observed to be about -21‰ δ^{13}C, which is 4.4 ‰ heavier than the biologically produced CO_2 (Ehleringer et al., 2000).

Therefore, CO_2 composition of Zyryanka ice wedge may have been consists of an admixture of DIC- derived CO_2, biological CO_2, and soil CO_2, resulting in enriched δ^{13}C signature.

4.2.3. CH_4

Several microbial studies on carbon isotope analyses of methane (Whiticar, 1999; Rivkina et al., 2007; Koch et al., 2009) and on methanogenesis in arctic climates (Høj et al., 2005; Wagner et al., 2005; Metje and Frenzel, 2007) suggest that methane occluded within the shallow permafrost deposits is attributed to microbial activity. In this regard, carbon isotope signatures of methane allow us to determine the possible origin of methane stored in the Zyryanka ice wedge.

According to Figure 4 in Whiticar (1999), relatively depleted carbon isotope value of CH_4 (δ^{13}C-CH_4) of Zyryanka ice wedge measured at an average of -69.3 ‰ (*n*=2) can be inferred

that origin of CH_4 gas within the ice wedge is bacterial, rather than thermogenic. Although there is no measured $\delta D\text{-}CH_4$ data for our samples, it can be clearly determined that origin of CH_4 in ice wedge is of bacterial whose $\delta^{13}C\text{-}CH_4$ ranges from -110 to -50 ‰, whereas thermogenic origin has a more enriched $\delta^{13}C\text{-}CH_4$ value range from roughly -50 to -20 ‰ (Whiticar, 1999). For this reason, it can be deduced that CH_4 was produced independently of CO_2, contrary to results of Kim et al. (2019) which argued that CO_2 and CH_4 are negatively correlated by processes produced (consumed) by methanogen and methanotrophs. Moreover, as I discussed section 4.2.1, fractionation factors of $CO_2\text{-}CH_4$ (ε_C) for Zyryanka ice wedge determined as 49.8 ± 2 (mean ± 1σ) imply that methane dominantly formed by methyl-type fermentation, rather than methane oxidation.

Interestingly, CH_4 composition of Zyryanka ice wedge was measured three or four orders of magnitude higher than that of LGP ice wedge samples located in central Yakutia, Siberia (Churapcha, Cyuie and Syrdakh; Kim et al., 2019; Yang et al., 2023) (Table 2 and Figure 10).

The main difference between the Zyryanka ice wedge and Churapcha, Cyuie and Syrdakh ice wedge is their formation age. The latter three ice wedges formed during the early Holocene and last glacial period, whereas Zyryanka ice wedge formed in the late Holocene, implying that different climatic conditions depending on age may have affected degree of methane production in different ice wedges.

Wagner et al. (2007) studied about Holocene permafrost deposits from the Lena River Delta in Siberia and observed enormous amounts of methane, which could be attributed to *in situ* activity of methanogenic bacteria. Furthermore, Bischoff et al. (2013) presented permafrost stratigraphic sequence of Late Pleistocene and Holocene deposits from Lena River Delta. This study noticed the quantitative and qualitative variation in the methanogenic communities in permafrost sediments formed under different climatic conditions, and impact of past climate

changes on the methane production. The Late Holocene paleoclimate of the Siberian Arctic is characterized by warmer and wet winter conditions (Wetterich et al., 2008), leading to remarkable increase in the abundance of methanogenic archaea communities compared to Late Pleistocene and Early Holocene deposits (Bischoff et al., 2013). Moreover, life marker analyses performed by Bischoff et al. (2013) also demonstrated that living microorganisms were more prevailed in Holocene deposits than Pleistocene one. Consequently, temperate environmental conditions of Late Holocene accompanying climate-driven response of methanogenic species as well as abundant living microorganisms are compatible with the elevated methane composition in Late Holocene deposits. In this context, it is likely to contain more living microorganisms within the Zyryanka ice wedge formed in the Late Holocene, implying that methanogenic archaea in the Zyryanka ice wedge deposits may have produced methane up to recently. However, it is far beyond the scope of this study to carry out detailed microbial sequencing for identifying origin of methane. To provide a clearer insight, future studies should extract DNA data to obtain more critical evidence whether methanogenic activity was persist for CH_4 production.

Meanwhile, one precondition for biological metabolism in frozen permafrost deposits is the availability of liquid water. Formation of Zyryanka ice wedge is characterized by mixing of liquid water and hoarfrost, so that liquid water within the ice wedge ice may have played important role in supplying the nutrients and ions to living methanogenic microorganisms. The hypothesis that liquid water from contact with active layer soil can also explain the CH_4 composition of ice wedge. Soil-derived water containing various nutrients is more advantageous for microbial activity, and CH_4 originated from active layer soil is also dissolved in liquid water, so that its chemical composition can be sufficiently reflected in the ice wedge.

In summary, to the best of our knowledge, it can be possible to present the origin of methane

and the possible explanation of the elevated methane composition in Zyryanka ice wedge.

4.2.4. N_2O

The N_2O composition of Zyryanka ice wedge with a mean of 3.28 ppm demonstrate an order of magnitude higher than that of Holocene atmospheric mixing ratio with a mean of 0.26 ppm N_2O. Compared to the N_2O mixing ratio of LGP ice wedges at central Yakutia, Siberia (mean of 1.27ppm for Cyuie sample and 3.33 ppm for Syrdakh samples, respectively; Kim et al., 2019; Yang et al., 2023), Zyryanka value is observed similar except for relatively higher values of Churapcha samples (140 ppm N_2O; Yang et al., 2023).

According to the negative $\delta(N_2/Ar)$ values of Zyryanka ice wedge, which is indicative of liquid water mixing, it can be considered reliable cause for elevated N_2O that snow/ice meltwater produced during or after the ice wedge formation.

Using the reported theoretical N_2O gas solubilities in Fogg and Sangster (2003), N_2O composition of the ice experienced partial melting or re-frozen with liquid water can be elevated up to ~11 ppm under 0°C and 1 atm condition. It can be observed that strong positive correlation between N_2O and liquid water fraction ($r=0.87$ and $p<0.05$) and that gas distribution profile from which the gas dissolution effect was removed is clearly deviated from the measured gas distribution profile (Figure 4). This can be obviously implied that liquid water contributed significantly to the alteration of N_2O composition of ice wedge.

Another possible physical process to modify the original N_2O gas composition is gas diffusion from adjacent permafrost soil to ice wedge. While it can be possible to estimate effect of diffusion using permeation coefficient (=diffusion coefficient * solubility) approximatively as introduced Kim et al. (2019), this cannot be clearly constrained for N_2O, unlike CO_2 and CH_4. Alternatively, coefficient of variation defined as Z-value (standard deviation/average) can be

calculated for identifying whether the gas diffusion play a significant role. I obtained and compared each z-values of CO_2 (0.17), CH_4 (0.78) and N_2O (1.01), which shows that the values for N_2O are relatively higher. Therefore, I cannot fully rule out the potential gas alteration by N_2O diffusion from soil to ice wedge ice.

On the other hands, biological contribution on producing excess N_2O can be considered as well. However, I speculated that N_2O production by microorganic metabolism is minor importance, given the major ion concentration measured below the detection limit. In natural permafrost condition, N_2O is usually produced via microbial nitrification oxidizing NH_4+ and denitrification reducing NO_3- (Ma et al., 2007; Palmer and Horn, 2012). To verify the biological contribution on the N_2O composition, these two major ion concentrations were measured using some ice wedge subsamples (n=7), and all the measured data results were obtained below detection limit (0.001 mg/L).

Given the mean N_2O composition of 3.28 ppm and the mean air contents (0.0273 mL/g_{ice}) of Zyryanka ice wedge samples, it can be estimated that 10.07mg/L for NO_3- and 2.92 mg/L for NH_4+ are required for N_2O production. These requirements are much greater than the measured ion concentration, indicating the depletion of both NO_3- and NH_4+ is not sufficient to elucidate the elevated N_2O composition within the ice wedge. Nevertheless, it cannot be ruled out the possibility of biological contribution to N_2O composition because existing ions within the ice wedge which get involved in nitrification/denitrification processes may have already been consumed to produce N_2O or N_2. Therefore, it can be inferred that abiotic process (in this study case, partial meltwater freezing) played a significant role in altered N_2O composition of ice wedge, unlike CO_2 and CH_4 which are dominantly affected by biological activity. The observation above implies that the N_2O mixing ratio of Zyryanka ice wedge resulted from a combination of physical modification process (gas dissolution in liquid water) and biological

respiration.

4.3. Relationship among three GHGs

I found that different pairs of three greenhouse gases and oxygen exhibit meaningful correlations. On the other hand, O_2 is negatively correlated with CO_2 and CH_4 ($r= -0.80$, $p <0.05$ and $r= -0.41$, $p< 0.05$, respectively, Figure 4), whereas there is no meaningful correlation between N_2O and O_2. It can be interpreted that O_2 might be consumed by microorganic respiration within the ice. Rivkina et al. (1998), Margesin (1999) and Cavicchioli (2006) reported cold-hardy microbial species present in permafrost environments, which may have consumed oxygen and produced methane and carbon dioxide in the ice wedge.

In the Brouchkov and Fukuda (2002) and Kim et al. (2019), they observed the negative correlations between the CO_2 and CH_4 concentrations, supporting the aerobic CH_4 oxidation process which led to the CO_2 production within the ice wedge. However, as I observed the carbon isotope fractionation factor (ε_C) between CO_2 and CH_4 in Zyryanka ice wedge (with the values of 49.8), our results imply that methanogenesis in ice wedge ice was occurred by methyl fermentation in freshwater condition, rather than methane oxidation. Moreover, CO_2 and CH_4 correlation in the Zyryanka ice wedge is not significant ($R^2=0.05$, $p<0.005$) (Figure 4), even though they clearly show the presence of oxygen in the ice given that the mean $\delta(O_2/Ar)$ values of -51.6% which indicates the selective loss of O_2. Therefore, our results are not consistent with previous study that clearly shows negative correlation between CO_2 and CH_4, which is indicative of CH_4 oxidation for CO_2 production.

I therefore speculated the reason for minor correlation of CO_2-CH_4 is that (1) anaerobic condition were established locally within the ice wedge in microscale, activating methanogenesis in given O_2-restricted environment and/ or (2) neither of the production/ consumption processes of CO_2 or CH_4 in terms of methanogenesis mechanisms prevailed.

For more detailed mechanisms on the latter, two main methanogenesis pathways can be considered under anaerobic condition. Acetoclastic methanogens can use acetate as substrate to produce CH_4 and CO_2 simultaneously (Conrad., 1999), which is predominant in the Arctic and subarctic permafrost condition (Metje and Frenzel, 2007). Meanwhile, hydrogentrophic methanogens convert CO_2 into CH_4 and H_2O, which is common in nutrient-poor peatland (Galand et al., 2010). Therefore, the production and consumption of CO_2 and CH_4 can depend on the relative contribution of the methanogenetic pathways mentioned above, inferring that lack of significant correlation of CO_2-CH_4 is due to both pathways occurred together.

On the other hand, N_2O and CO_2 shows a strong positive correlation ($r = 0.94$, $p < 0.05$), whereas weak negative correlation is shown between N_2O and CH_4 ($r = -0.39$, $p = 0.04$).

Moreover, CO_2 and N_2O also shows close positive correlation with liquid water fraction respectively (R^2=0.6 and 0.7 for CO_2 and N_2O, respectively), which indicates that both greenhouse gas compositions are obviously affected by liquid water presence.

4.4. Comparison of GHGs distribution with other ice wedges

Another noticeable result of this study is the specific relationship of GHGs mixing ratios among different ice wedges as already discussed in Kim et al. (2019) and Yang et al. (2023). Previous study observed a remarkable signature in the relationship of the CH_4 and N_2O mixing ratios in two ice-wedge outcrops in Cyuie, Central Yakutia (Kim et al., 2019). The Cyuie CH_4 and N_2O mixing ratios exhibited a clear “L-shaped” distribution, in that the ice-wedge samples elevated in CH_4 were depleted in N_2O mixing ratios and vice versa. This indicates that CH_4 and N_2O cannot be enriched simultaneously; therefore, some inhibitory effects should play an important role in the CH_4^- and N_2O^- producing pathways. Furthermore, in the CO_2-CH_4 relationship, Zyryanka ice wedge samples show similar ranges of CO_2 mixing ratios, while the CH_4 was measured approximately three orders of magnitude higher than that of other Siberian ice

wedges.

Chapter 5. Conclusion

GHGs, Ar-O_2-N_2 gas mixing ratio along with detailed water chemistry analysis of Zyryanka ice wedge in this study allowed us to shed more light on the ice wedge formation mechanisms and origin of gas species. Zyryanka ice wedge study has the advantage of simultaneously analyzing various chemical parameters of only one ice wedge sample at a given study site and verifying close correlation to increase the spatial resolution of the ice wedge study.

Zyryanka ice wedge was formed in the late Holocene of 1.3 ka. The N_2/Ar mixing ratio ($\delta(N_2/Ar)$) and bubble shapes indicate that this ice wedge mainly formed by mixing of dry snow and liquid water, rather than only dry snow (or hoarfrost) compaction. According to higher GHGs composition compared to the late Holocene atmospheric level, and the correlation of each gas composition of ice wedge, I can suggest that in situ microbial activity within the ice wedge and influence of soil water. Furthermore, it was inferred that additional dissolution of soil-derived gas may occur by infiltration of liquid water, which could modify the original gas composition of ice wedge.

For the ice wedge and precipitation co-isotope relationship, it can be observed that the $\delta^{18}O$-δD regression slope of Zyryanka ice wedge ($\delta D = 7.24 * \delta^{18}O - 15.16$) is very close to that of local meteoric water line of Zyryanka region (LMWL, $\delta D = 7.46 * \delta^{18}O - 9.24$). It can be accordingly inferred that the ice wedge has experienced little secondary isotope fractionation. Meanwhile, comparing with the $\delta^{18}O$ value of modern precipitation in the Zyryanka region, it can be inferred that winter precipitation from October to April mainly contributed to the formation of the Zyryanka ice wedge.

Furthermore, it should be noticed the effect of surrounding impurities that can alter the original chemistry of ice wedge, which cause uncertainty of ice wedge as a winter paleoclimate proxy. However, because no significant isotopic alteration by neighboring soils was observed in

Zyryanka ice wedge, implying that paleoclimate signature of Zyryanka ice wedge remain well-preserved, so that this ice wedge can play an important role as a paleoclimate proxy.

References

Bauska, T. K., Joos, F., Mix, A. C., Roth, R., Ahn, J., & Brook, E. J. (2015). Links between atmospheric carbon dioxide, the land carbon reservoir and climate over the past millennium. *Nature Geoscience*, 8(5), 383-387. https://doi.org/10.1038/ngeo2422

Beria, H., Larsen, J. R., Ceperley, N. C., Michelon, A., Vennemann, T., & Schaefli, B. (2018). Understanding snow hydrological processes through the lens of stable water isotopes. *WIREs Water*, 5(6), e1311. https://doi.org/https://doi.org/10.1002/wat2.1311

Boereboom, T., Depoorter, M., Coppens, S., & Tison, J. L. (2012). Gas properties of winter lake ice in Northern Sweden: implication for carbon gas release. *Biogeosciences*, *9*(2), 827-838. https://doi.org/10.5194/bg-9-827-2012

Boereboom, T., Samyn, D., Meyer, H., & Tison, J. L. (2013). Stable isotope and gas properties of two climatically contrasting (Pleistocene and Holocene) ice wedges from Cape Mamontov Klyk, Laptev Sea, northern Siberia. *The Cryosphere*, 7(1), 31-46. https://doi.org/10.5194/tc-7-31-2013

Campbell-Heaton, K., Lacelle, D., & Fisher, D. (2021). Ice wedges as winter temperature proxy: Principles, limitations and noise in the $\delta^{18}O$ records (an example from high Arctic Canada). *Quaternary Science Reviews*, 269, 107135. https://doi.org/https://doi.org/10.1016/j.quascirev.2021.107135

Campeau, A., Wallin, M. B., Giesler, R., Löfgren, S., Mörth, C.-M., Schiff, S., Venkiteswaran, J. J., & Bishop, K. (2017). Multiple sources and sinks of dissolved inorganic carbon across Swedish streams, refocusing the lens of stable C isotopes. *Scientific Reports*, 7(1), 9158. https://doi.org/10.1038/s41598-017-09049-9

Cardyn, R., Clark, I. D., Lacelle, D., Lauriol, B., Zdanowicz, C., & Calmels, F. (2007). Molar gas ratios of air entrapped in ice: A new tool to determine the origin of relict massive ground ice bodies in permafrost. *Quaternary Research*, *68*(2), 239-248. <Go to ISI>://WOS:000249281600008

Cavicchioli, R. (2006). Cold-adapted archaea. Nature Reviews Microbiology, 4(5), 331-343. https://doi.org/10.1038/nrmicro1390

Cerling, T. E., Harris, J. M., MacFadden, B. J., Leakey, M. G., Quade, J., Eisenmann, V., & Ehleringer, J. R. (1997). Global vegetation change through the Miocene/Pliocene boundary. *Nature*, 389(6647), 153-158. https://doi.org/10.1038/38229

Cerling, T. E., Wang, Y., & Quade, J. (1993). Expansion of C4 ecosystems as an indicator of global ecological change in the late Miocene. *Nature*, 361(6410), 344-345. https://doi.org/10.1038/361344a0

Cerling, T. E., Solomon, D. K., Quade, J., & Bowman, J. R. (1991). On the isotopic composition of carbon in soil carbon dioxide. *Geochimica et Cosmochimica Acta*, 55(11), 3403-3405. https://doi.org/https://doi.org/10.1016/0016-7037(91)90498-T

Conrad, R. (1999). Contribution of hydrogen to methane production and control of hydrogen concentrations in methanogenic soils and sediments. *FEMS Microbiology Ecology*, 28(3), 193-202. https://doi.org/10.1111/j.1574-6941.1999.tb00575.x

Coplen, T. B., Coplen, T. B., & Peiser, H. S. (2002). Compilation of minimum and maximum isotope ratios of selected elements in naturally occurring terrestrial materials and reagents. U.S. Dept. of the Interior, U.S. Geological Survey. http://hdl.handle.net/2027/mdp.39015055598166

Craig, H. (1961). Isotopic variations in meteoric waters. *Science*, 133(3465), 1702–1703.

Dansgaard W. 1964. Stable isotopes in precipitation.Tellus16: 436 – 468

Dean, J. F., Meisel, O. H., Martyn Rosco, M., Marchesini, L. B., Garnett, M. H., Lenderink, H., van Logtestijn, R., Borges, A. V., Bouillon, S., Lambert, T., Röckmann, T., Maximov, T., Petrov, R., Karsanaev, S., Aerts, R., van Huissteden, J., Vonk, J. E., & Dolman, A. J. (2020). East Siberian Arctic inland waters emit mostly contemporary carbon. *Nature Communications*, 11(1), 1627. https://doi.org/10.1038/s41467-020-15511-6

Doctor, D. H., Kendall, C., Sebestyen, S. D., Shanley, J. B., Ohte, N., & Boyer, E. W. (2008). Carbon isotope fractionation of dissolved inorganic carbon (DIC) due to outgassing of carbon dioxide from a headwater stream. *Hydrological Processes*, 22(14), 2410-2423. https://doi.org/https://doi.org/10.1002/hyp.6833

Ehleringer, J. R., Buchmann, N., & Flanagan, L. B. (2000). CARBON ISOTOPE RATIOS IN BELOWGROUND CARBON CYCLE PROCESSES. *Ecological Applications*, 10(2), 412-422. https://doi.org/https://doi.org/10.1890/1051-0761(2000)010[0412:CIRIBC]2.0.CO;2

Fedorov, A. N., Ivanova, R. N., Park, H., Hiyama, T., & Iijima, Y. (2014). Recent air temperature changes in the permafrost landscapes of northeastern Eurasia. *Polar Science*, *8*(2), 114-128. https://doi.org/10.1016/j.polar.2014.02.001

Fedorov, A.N.; Botulu, T.A.; Vasiliev, I.S.; Varlamov, S.P.; Gribanova, S.P.; Dorofeev, I.V. Permafrost-Landscape Map of the Yakut ASSR, Scale 1:2,500,000, 2 Sheets; Melnikov, P.I., Ed.; Gosgeodezia: Moscow, Russia, 1991

Fogg, P. G. T., Sangster, J., International Union of, P., & Applied Chemistry. Commission on Solubility, D. (2003). Chemicals in the atmosphere : solubility, sources, and reactivity. J. Wiley. http://catdir.loc.gov/catdir/toc/wiley032/2003053494.html

Galand, P. E., Yrjälä, K., & Conrad, R. (2010). Stable carbon isotope fractionation during methanogenesis in three boreal peatland ecosystems. *Biogeosciences*, 7(11), 3893-3900. https://doi.org/10.5194/bg-7-3893-2010

Galanin A.A. (2021). About the incorrectness of Yu.K. Vasil'chuk's method for the reconstruction of paleotemperatures using isotope composition of wedge ice. Review of the article by Yu.K. Vasil'chuk, A.C. Vasil'chuk "Air January paleotemperature reconstruction 48–15 calibrat. *Earth's Cryosphere*, 2, 62–75, DOI: 10.15372/KZ20210206 (in Russian with English summary).

Gibson, J. J., & Prowse, T. D. (2002). Stable isotopes in river ice: identifying primary over-winter streamflow signals and their hydrological significance. *Hydrological Processes*, 16(4), 873-890. https://doi.org/https://doi.org/10.1002/hyp.366

Gidrometeoizdat, Leningrad (1989). Handbook on the USSR climate. Series 3. Long-Term Data. Parts 1-6, *24*(1), 607 (in Russian)

Hirota, A., Tsunogai, U., Komatsu, D. D., & Nakagawa, F. (2010). Simultaneous determination of $\delta^{15}N$ and $\delta^{18}O$ of N_2O and $\delta^{13}C$ of CH_4 in nanomolar quantities from a single water sample. *Rapid Communications in Mass Spectrometry,* 24(7), 1085-1092. https://doi.org/https://doi.org/10.1002/rcm.4483

Høj, L., Olsen, R. A., & Torsvik, V. L. (2005). Archaeal communities in High Arctic wetlands at Spitsbergen, Norway (78 degrees N) as characterized by 16S rRNA gene fingerprinting. *FEMS Microbiol Ecol*, 53(1), 89-101. https://doi.org/10.1016/j.femsec.2005.01.004

Holland, H. D. (1984). The chemical evolution of atmosphere and oceans. Princeton University Press.

Ichiyanagi, K., Suwarman, R., Belgaman, H. A., Tanoue, M., Uesugi, T., & Warjono. (2019). Diurnal variation of stable isotopes in rainfall observed at Bengkulu for the YMC-Sumatra 2017. *International Conference on Tropical Meteorology and Atmospheric Sciences*, 303. https://doi.org/Artn 01200810.1088/1755-1315/303/1/012008

Jouzel, J. (2003). Water Stable Isotopes: Atmospheric Composition and Applications in Polar Ice Core Studies. In H. D. Holland & K. K. Turekian (Eds.), *Treatise on Geochemistry* (pp. 213-243). Pergamon. https://doi.org/https://doi.org/10.1016/B0-08-043751-6/04040-8

Kawagucci, S., Tsunogai, U., Kudo, S., Nakagawa, F., Honda, H., Aoki, S., Nakazawa, T., & Gamo, T. (2005). An Analytical System for Determining $\delta^{17}O$ in CO_2 Using Continuous Flow-Isotope Ratio MS. *Analytical Chemistry*, 77(14), 4509-4514. https://doi.org/10.1021/ac050266u

Kim, K., Yang, J. W., Yoon, H., Byun, E., Fedorov, A., Ryu, Y., & Ahn, J. (2019). Greenhouse gas formation in ice wedges at Cyuie, central Yakutia. *Permafrost and Periglacial Processes*, *30*(1), 48-57. https://doi.org/10.1002/ppp.1994

Koch, K., Knoblauch, C., & Wagner, D. (2009). Methanogenic community composition and anaerobic carbon turnover in submarine permafrost sediments of the Siberian Laptev Sea. *Environ Microbiol*, 11(3), 657-668. https://doi.org/10.1111/j.1462-2920.2008.01836.x

Koshkarova, V. L., & Koshkarov, A. D. (2004). Regional signatures of changing landscape and climate of northern Central Siberia in the Holocene. *Geologiya i Geofizika*, 45, 717-729.

Kurita, N., Yoshida, N., Inoue, G., & Chayanova, E. A. (2004). Modern isotope climatology of Russia: A first assessment. *Journal of Geophysical Research: Atmospheres*, 109(D3). https://doi.org/https://doi.org/10.1029/2003JD003404

Lacelle, D. (2011a). On the $\delta^{18}O$, δD and D-excess relations in meteoric precipitation and during equilibrium freezing: theoretical approach and field examples. *Permafrost and Periglacial Processes*, 22(1), 13-25. https://doi.org/https://doi.org/10.1002/ppp.712

Lacelle, D., Radtke, K., Clark, I. D., Fisher, D., Lauriol, B., Utting, N., & Whyte, L. G. (2011b). Geomicrobiology and occluded O_2–CO_2–Ar gas analyses provide evidence of microbial respiration in ancient terrestrial ground ice. *Earth and Planetary Science Letters*, 306(1), 46-54. https://doi.org/https://doi.org/10.1016/j.epsl.2011.03.023

Land, L. S., Zenger, D. H., Dunham, J. B., & Ethington, R. L. (1980). The Isotopic and Trace Element Geochemistry of Dolomite: The State of the Art. *Concepts and Models of Dolomitization* (Vol. 28, pp. 0). SEPM Society for Sedimentary Geology. https://doi.org/10.2110/pec.80.28.0087

Laonamsai, J., Ichiyanagi, K., Kamdee, K., Putthividhya, A., & Tanoue, M. (2021). Spatial and temporal distributions of stable isotopes in precipitation over Thailand. *Hydrological Processes*, 35(1), e13995. https://doi.org/https://doi.org/10.1002/hyp.13995

Lauriol, B., Lacelle, D., St-Jean, M., Clark, I. D., & Zazula, G. D. (2010). Late Quaternary paleoenvironments and growth of intrusive ice in eastern Beringia (Eagle River valley, northern Yukon, Canada). *Canadian Journal of Earth Sciences*, *47*(7), 941-955. https://doi.org/10.1139/E10-012

Ma, W. K., Schautz, A., Fishback, L.-A. E., Bedard-Haughn, A., Farrell, R. E., & Siciliano, S. D. (2007). Assessing the potential of ammonia oxidizing bacteria to produce nitrous oxide in soils of a high arctic lowland ecosystem on Devon Island, Canada. *Soil Biology and Biochemistry*, 39(8), 2001-2013. https://doi.org/https://doi.org/10.1016/j.soilbio.2007.03.001

Lüttge U. (2010). Ability of crassulacean acid metabolism plants to overcome interacting stresses in tropical environments. *AoB PLANTS*, 2010, plq005. https://doi.org/10.1093/aobpla/plq005

MACKAY, J. R. (1972). THE WORLD OF UNDERGROUND ICE. *Annals of the Association of American Geographers*, *62*(1), 1-22. https://doi.org/https://doi.org/10.1111/j.1467-8306.1972.tb00839.x

Mackay, J. R. (1983). Oxygen Isotope Variation in Permafrost, Tuktoyaktuk Peninsula area, Northwest Territories.

Margesin, R. (1999). Cold-adapted organisms: Ecology, physiology, enzymology and molecular biology. Springer Science & Business Media.

Metje, M., & Frenzel, P. (2007). Methanogenesis and methanogenic pathways in a peat from subarctic permafrost. *Environmental Microbiology*, 9(4), 954-964. https://doi.org/https://doi.org/10.1111/j.1462-2920.2006.01217.x

Meyer, H., Dereviagin, A., Siegert, C., Schirrmeister, L., & Hubberten, H.-W. (2002). Palaeoclimate reconstruction on Big Lyakhovsky Island, north Siberia—hydrogen and oxygen isotopes in ice wedges. *Permafrost and Periglacial Processes*, 13(2), 91-105. https://doi.org/https://doi.org/10.1002/ppp.416

Meyer, H., Yu, A., & Hubberten, H.-W. (2007). Paleoelimate Studies on Bykovsky Peninsula , North Siberia Hydrogen and Oxygen Isotopes in Ground lee.

Meyer, H., Schirrmeister, L., Andreev, A., Wagner, D., Hubberten, H.-W., Yoshikawa, K., Bobrov, A., Wetterich, S., Opel, T., Kandiano, E., & Brown, J. (2010a). Lateglacial and Holocene isotopic and environmental history of northern coastal Alaska – Results from a buried ice-wedge system at Barrow. *Quaternary Science Reviews*, 29(27), 3720-3735. https://doi.org/https://doi.org/10.1016/j.quascirev.2010.08.005

Meyer, H., Schirrmeister, L., Yoshikawa, K., Opel, T., Wetterich, S., Hubberten, H.-W., & Brown, J. (2010b). Permafrost evidence for severe winter cooling during the Younger Dryas in northern Alaska. *Geophysical Research Letters*, 37(3). https://doi.org/https://doi.org/10.1029/2009GL041013

Meyer, H., Opel, T., Laepple, T., Dereviagin, A. Y., Hoffmann, K., & Werner, M. (2015). Long-term winter warming trend in the Siberian Arctic during the mid- to late Holocene. *Nature Geoscience*, 8(2), 122-125. https://doi.org/10.1038/ngeo2349

Meyer, H., Kostrova, S. S., Meister, P., Lenz, M. M., Kuhn, G., Nazarova, L., Syrykh, L. S., & Dvornikov, Y. (2022). Lacustrine diatom oxygen isotopes as palaeo precipitation proxy - Holocene environmental and

snowmelt variations recorded at Lake Bolshoye Shchuchye, Polar Urals, Russia. *Quaternary Science Reviews*, 290, 107620. https://doi.org/https://doi.org/10.1016/j.quascirev.2022.107620

Miller, G. H., Brigham-Grette, J., Alley, R. B., Anderson, L., Bauch, H. A., Douglas, M. S. V., Edwards, M. E., Elias, S. A., Finney, B. P., Fitzpatrick, J. J., Funder, S. V., Herbert, T. D., Hinzman, L. D., Kaufman, D. S., MacDonald, G. M., Polyak, L., Robock, A., Serreze, M. C., Smol, J. P., . . . Wolff, E. W. (2010). Temperature and precipitation history of the Arctic. *Quaternary Science Reviews*, 29(15), 1679-1715. https://doi.org/https://doi.org/10.1016/j.quascirev.2010.03.001

Nikolayev, V. I., & Mikhalev, D. V. (1995). An Oxygen-Isotope Paleothermometer from Ice in Siberian Permafrost. *Quaternary Research*, 43(1), 14-21. https://doi.org/https://doi.org/10.1006/qres.1995.1002

Oleary, M. H. (1981). Carbon Isotope Fractionation in Plants. *Phytochemistry*, *20*(4), 553-567. <Go to ISI>://WOS:A1981LP76300001

Opel, T., Dereviagin, A. Y., Meyer, H., Schirrmeister, L., & Wetterich, S. (2011). Palaeoclimatic Information from Stable Water Isotopes of Holocene Ice Wedges on the Dmitrii Laptev Strait, Northeast Siberia, Russia. *Permafrost and Periglacial Processes*, *22*(1), 84-100. https://doi.org/10.1002/ppp.667

Opel, T., Wetterich, S., Meyer, H., Dereviagin, A. Y., Fuchs, M. C., & Schirrmeister, L. (2017). Ground-ice stable isotopes and cryostratigraphy reflect late Quaternary palaeoclimate in the Northeast Siberian Arctic (Oyogos Yar coast, Dmitry Laptev Strait). *Clim. Past*, 13(6), 587-611. https://doi.org/10.5194/cp-13-587-2017

Opel, T., Murton, J. B., Wetterich, S., Meyer, H., Ashastina, K., Günther, F., Grotheer, H., Mollenhauer, G., Danilov, P. P., Boeskorov, V., Savvinov, G. N., & Schirrmeister, L. (2019). Past climate and continentality inferred from ice wedges at Batagay megaslump in the Northern Hemisphere's most continental region, Yana Highlands, interior Yakutia. *Clim. Past*, 15(4), 1443-1461. https://doi.org/10.5194/cp-15-1443-2019

Palmer, K., & Horn, M. A. (2012). Actinobacterial Nitrate Reducers and Proteobacterial Denitrifiers Are Abundant in N_2O-Metabolizing Palsa Peat. *Applied and Environmental Microbiology*, 78(16), 5584-5596. https://doi.org/doi:10.1128/AEM.00810-12

"Pogodaiklimat, world climate, Zyryanka." Pogodaiklimat. last modified Nov 03, 2022, accessed Nov 03, 2022, http://pogodaiklimat.ru/climate/25400.htm

Popp, S., Diekmann, B., Meyer, H., Siegert, C., Syromyatnikov, I., & Hubberten, H.-W. (2006). Palaeoclimate signals as inferred from stable-isotope composition of ground ice in the Verkhoyansk foreland, Central Yakutia. *Permafrost and Periglacial Processes*, 17(2), 119-132. https://doi.org/https://doi.org/10.1002/ppp.556

Porter, T. J., Froese, D. G., Feakins, S. J., Bindeman, I. N., Mahony, M. E., Pautler, B. G., Reichart, G.-J., Sanborn, P. T., Simpson, M. J., & Weijers, J. W. H. (2016). Multiple water isotope proxy reconstruction of extremely low last glacial temperatures in Eastern Beringia (Western Arctic). *Quaternary Science Reviews*, 137, 113-125. https://doi.org/https://doi.org/10.1016/j.quascirev.2016.02.006

Porter, T. J., & Opel, T. (2020). Recent advances in paleoclimatological studies of Arctic wedge- and pore-ice stable-water isotope records. Permafrost and Periglacial Processes, 31(3), 429-441. https://doi.org/https://doi.org/10.1002/ppp.2052

Raghavendra, A. S., Raghavendra, A. S., Sage, R. F., & SpringerLink. (2011). C_4 Photosynthesis and Related CO_2 Concentrating Mechanisms (1st 2011. ed.). Springer Netherlands : Imprint: Springer.https://www.bath.ac.uk/library/openurl/?u.ignore_date_coverage=true&rft.mms_id=991003542426902761

Rivkina, E., Gilichinsky, D., Wagener, S., Tiedje, J., & McGrath, J. (1998). Biogeochemical activity of anaerobic microorganisms from buried permafrost sediments. *Geomicrobiology Journal*, *15*(3), 187-193. https://doi.org/10.1080/01490459809378075

Rivkina, E., Shcherbakova, V., Laurinavichius, K., Petrovskaya, L., Krivushin, K., Kraev, G., Pecheritsina, S., & Gilichinsky, D. (2007). Biogeochemistry of methane and methanogenic archaea in permafrost. *FEMS Microbiology Ecology*, 61(1), 1-15. https://doi.org/10.1111/j.1574-6941.2007.00315.x

Rochette, P., & Flanagan, L. B. (1997). Quantifying Rhizosphere Respiration in a Corn Crop under Field Conditions. *Soil Science Society of America Journal*, 61(2), 466-474. https://doi.org/https://doi.org/10.2136/sssaj1997.03615995006100020014x

Rozanski, K., Araguás-Araguás, L., & Gonfiantini, R. (1993). Isotopic Patterns in Modern Global Precipitation. In *Climate Change in Continental Isotopic Records* (pp. 1-36). https://doi.org/https://doi.org/10.1029/GM078p0001

Rubino, M., Etheridge, D. M., Thornton, D. P., Howden, R., Allison, C. E., Francey, R. J., Langenfelds, R. L., Steele, L. P., Trudinger, C. M., Spencer, D. A., Curran, M. A. J., van Ommen, T. D., & Smith, A. M. (2019). Revised records of atmospheric trace gases CO_2, CH_4, N_2O, and $\delta^{13}C$-CO_2 over the last 2000 years from Law Dome, Antarctica. *Earth Syst. Sci. Data*, *11*(2), 473-492. https://doi.org/10.5194/essd-11-473-2019

St-Jean, M., Lauriol, B., Clark, I. D., Lacelle, D., & Zdanowicz, C. (2011). Investigation of ice-wedge infilling processes using stable oxygen and hydrogen isotopes, crystallography and occluded gases (O_2, N_2, Ar). *Permafrost and Periglacial Processes*, *22*(1), 49-64. https://doi.org/https://doi.org/10.1002/ppp.680

Staddon, P. L. (2004). Carbon isotopes in functional soil ecology. *Trends in Ecology & Evolution*, 19(3), 148-154. https://doi.org/https://doi.org/10.1016/j.tree.2003.12.003

Strauss, J. (2010). Late Quaternary environmental dynamics at the Duvanny Yar key section, Lower Kolyma, East Siberia.

Streletskaya, I. D., Vasiliev, A. A., Oblogov, G. E., and Tokarev, I. V. (2015). Reconstruction of Paleoclimate of Russian Arctic in Late Pleistocene–Holocene on the Basis of Isotope Study of Ice Wedges. *Earth's Cryosphere*, 19 (2), 86-94.

Throckmorton, H. M., Heikoop, J. M., Newman, B. D., Altmann, G. L., Conrad, M. S., Muss, J. D., Perkins, G. B., Smith, L. J., Torn, M. S., Wullschleger, S. D., & Wilson, C. J. (2015). Pathways and transformations of dissolved methane and dissolved inorganic carbon in Arctic tundra watersheds: Evidence from analysis of stable isotopes. *Global Biogeochemical Cycles*, 29(11), 1893-1910. https://doi.org/https://doi.org/10.1002/2014GB005044

Vasil'chuk Y.K. (1993). Northern Asia cryolithozone evolution in Late Quaternary // Proceedings of the Sixth International Conference on Permafrost. Beijing, China. South China University of Technology Press, Wushan, Guangzhou. Vol. 1. pp. 945-950 Earth's Cryosphere. 19 (2), 86–94

Vasil'chuk, Y. K., & Budantseva, N. A. (2021). Holocene ice wedges of the Kolyma Lowland and January paleotemperature reconstructions based on oxygen isotope records. *Permafrost and Periglacial Processes*, *33*(1), 3-17. https://doi.org/10.1002/ppp.2128

Vaikmäe, R. (1990). Oxygen isotopes in permafrost and ground ice: A new tool for paleoclimatic investigations (pp. 543–553). Zentralinstitut für Isotopen und Strahlenforschung.

Whiticar, M. J. (1999). Carbon and hydrogen isotope systematics of bacterial formation and oxidation of methane. Chemical Geology, 161(1), 291-314. https://doi.org/https://doi.org/10.1016/S0009-2541(99)00092-3

Wilkie, K., Chapligin, B., Meyer, H., Burns, S., Petsch, S., & Brigham-Grette, J. (2012). Modern isotope hydrology and controls on δD of plant leaf waxes at Lake El'gygytgyn, NE Russia. *Climate of the Past Discussions*, 8, 3719-3764. https://doi.org/10.5194/cpd-8-3719-2012

Yang, J. W., Ahn, J., Iwahana, G., Han, S., Kim, K., & Fedorov, A. (2020). Brief Communication: The reliability of gas extraction techniques for analysing CH_4 and N_2O compositions in gas trapped in permafrost ice wedges. *The Cryosphere*, *14*(4), 1311-1324. https://doi.org/10.5194/tc-14-1311-2020

Yang, J.-W., Ahn, J., Iwahana, G., Ko, N., Kim, J.-H., Kim, K., Fedorov, A., & Han, S. (2023). Origin of CO_2, CH_4, and N_2O trapped in ice wedges in central Yakutia and their relationship. Permafrost and Periglacial Processes, 34(1), 122-141. https://doi.org/https://doi.org/10.1002/ppp.2176

국문초록

다중 지구 화학 분석은 얼음 쐐기 형성 과정과 현장 온실 가스(GHG) 생성 메커니즘을 더 잘 이해하는 데 도움이 될 수 있다. 본 논문에서는 북동 시베리아의 지랸카 지역 얼음 쐐기의 새로운 연구 결과를 제시한다. 방사성 탄소 연대 측정을 위해 식물 잔해와 얼음 쐐기에 포집된 CO_2 가스가 분석되었고, 그 연대는 얼음 쐐기의 경우 810년~1750년 (1950 CE 이전, 얼음 쐐기와 인접한 토양의 경우 평균 4220년(1950 CE 이전)으로 측정되었다. $\delta(N_2/Ar)$값은 현대 공기의 값을 기준으로 −17.51 ~ −3.53% 범위이며, 이는 액체 상태의 물과 서리가 함께 채워져 얼음 쐐기가 형성되었음을 나타낸다. 반면, 지랸카 얼음 쐐기의 $\delta(O_2/Ar)$ 값은 현대 공기의 값을 기준으로 −72.88 ~ −37.58% 범위이며, 이는 산소 가스가 얼음 쐐기 내의 미생물 호흡에 의해 선택적으로 소비되었음을 암시한다. 온실 가스 성분(CO_2, CH_4 및 N_2O)은 홀로세 대기 수준보다 몇 배 더 높게 나타난다. 본 연구에서 지구화학적 및 지구물리학적 분석을 통해 온실 가스가 대부분 미생물 활동에 의해 생성되었으나, 부분적으로는 액체 물에 용해된 가스에서 비롯되었음을 확인하였다. $\delta^{18}O$ 값은 얼음 쐐기와 인접한 토양 얼음에 대해 각각 −28.14 ± 0.39 및 −21.85 ± 1.96 ‰ (평균값 ± 1σ)이므로 인접한 토양에서 얼음 쐐기로 동위원소 확산이 없음을 의미한다. 지랸카 지역 현대 강수의 $\delta^{18}O$ 값과 비교하면, 얼음 쐐기는 주로 겨울 강수(10월부터 4월까지)에 의해 형성되었음을 추론할 수 있다. 또한, 기존의 고기온 복원 방정식의 신뢰성을 테스트했다. 본 연구는 얼음 쐐기의 가스 혼합 비율과 물 안정 동위원소 조성 분석을 통해 얼음 쐐기 형성 환경을 더 잘 이해할 수 있을 뿐만 아니라, 얼음 쐐기의 고기후 프록시로서의 신뢰성을 검증하는 데 도움이 될 수 있음을 시사한다.

주요어: 영구 동토층, 얼음 쐐기, 물 안정동위원소, 온실 가스, 가스 혼합비율, 북동시베리아

학번: 2020−28766

List of Figures

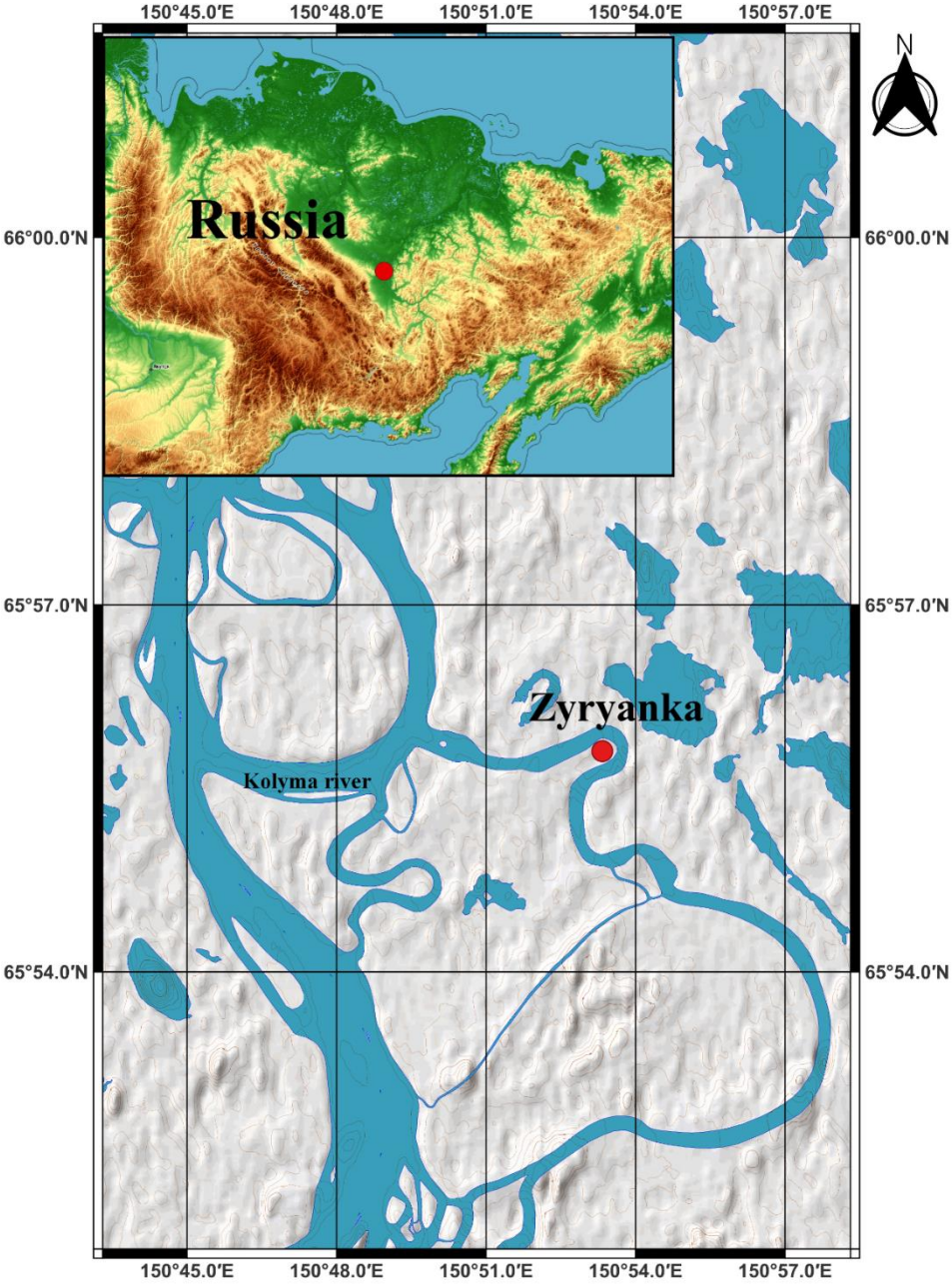

Figure 1. Map of the Zyryanka sampling site. The sampling site is located at near the Kolyma River. Site A is located a tributary of the Kolyma River about 22 km north from Zyryanka. Site B was about 14 km west from entrance of a tributary of Kolyma, which starts from about 11 km north of Zyryanka.

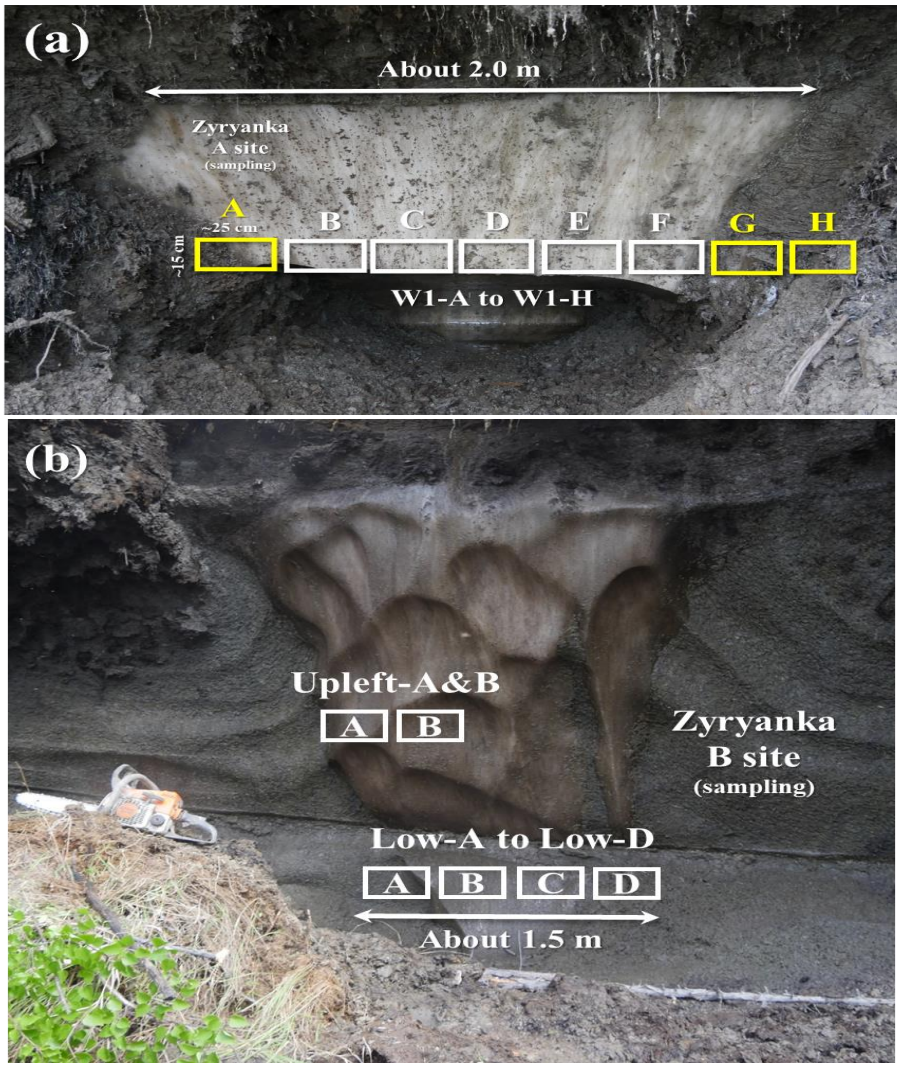

Figure 2. Overall view of Zyryanka A and B site ice wedge outcrop. Eight block samples(W1-A to W1-H) were taken horizontally at the 2.5 m depth (a). It should be noted that Wl-A, G and H samples are texture ice adjacent to the ice wedge and only from W1-B to F samples are the pure ice wedge part. Sediments abutting on W1 ice block comprise of silt, organic matter, plant residue, etc. Top of sampled ice wedge of site B started from about 1.2 m below the ground surface (b). Width of the ice-wedge top was about 2 m. The site B ice wedge was surrounded by highly ice-rich sediments with gray silt, which contains chunks of peaty organic matter sometimes with larger tree trunks. Block samples were collected horizontally from upper (B_UpLeft-1 and B_UpLeft-2) and lower (B-Low-A to B-Low-D) potion of the ice-wedge exposure.

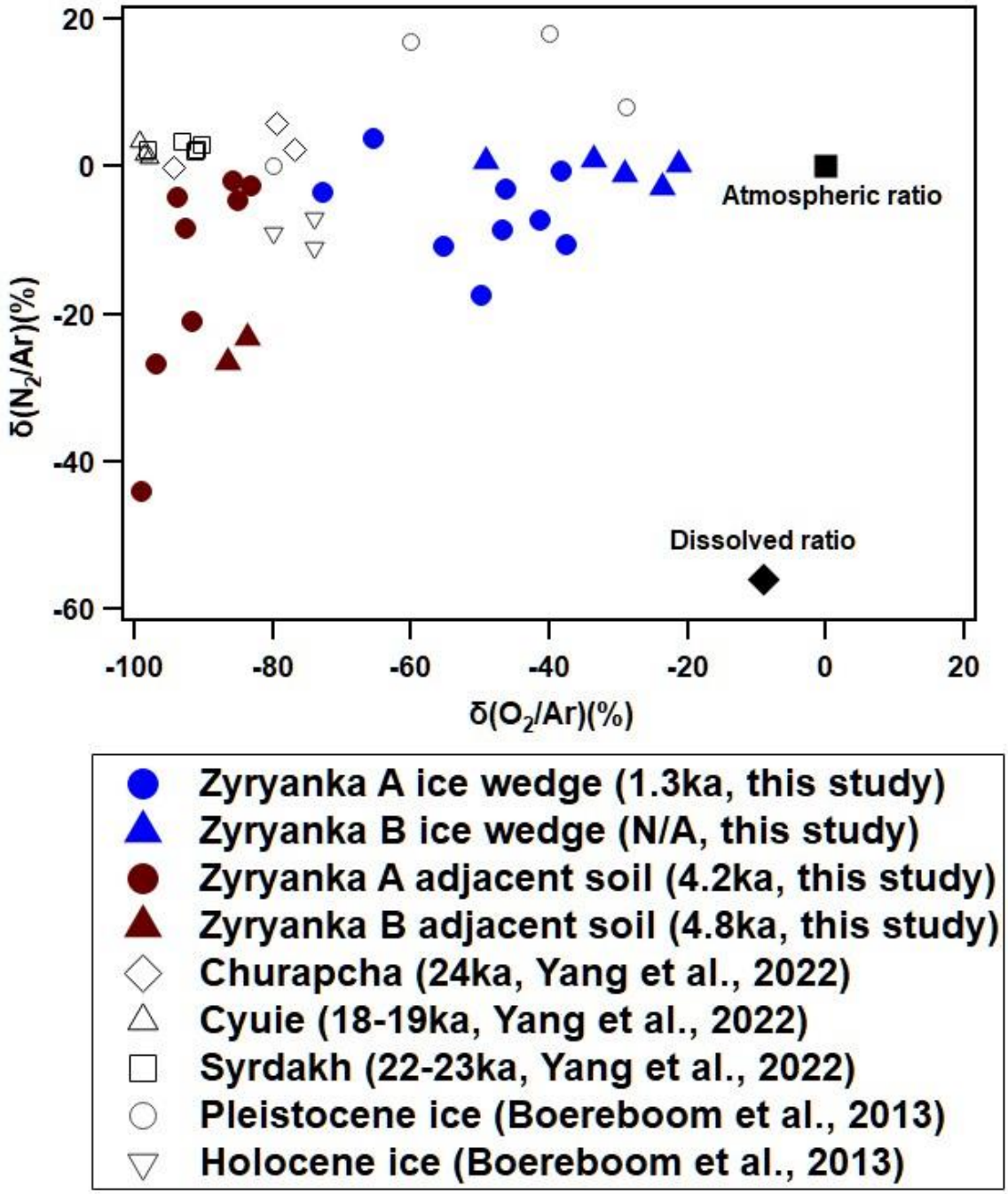

Figure 3. $\delta(N_2/Ar)$ and $\delta(O_2/Ar)$ mixing ratios of various ice wedges corresponding to different geologic ages. Black solid square is atmospheric composition and Black diamond reflects the composition of each gas completely dissolved in liquid water. Blue color symbol indicates Zyryanka A(circle) and B(triangle) ice wedge value, whereas the brown color symbol indicates soil value adjacent to each A and B ice wedge on both sides. Other hollow symbols represent ice wedge values in the Yakutsk region in Central Siberia formed in the Last Glacial Periods (Yang et a., 2022) and those near the Labtev sea region formed in the Pleistocene and Holocene (Boereboom et al., 2013).

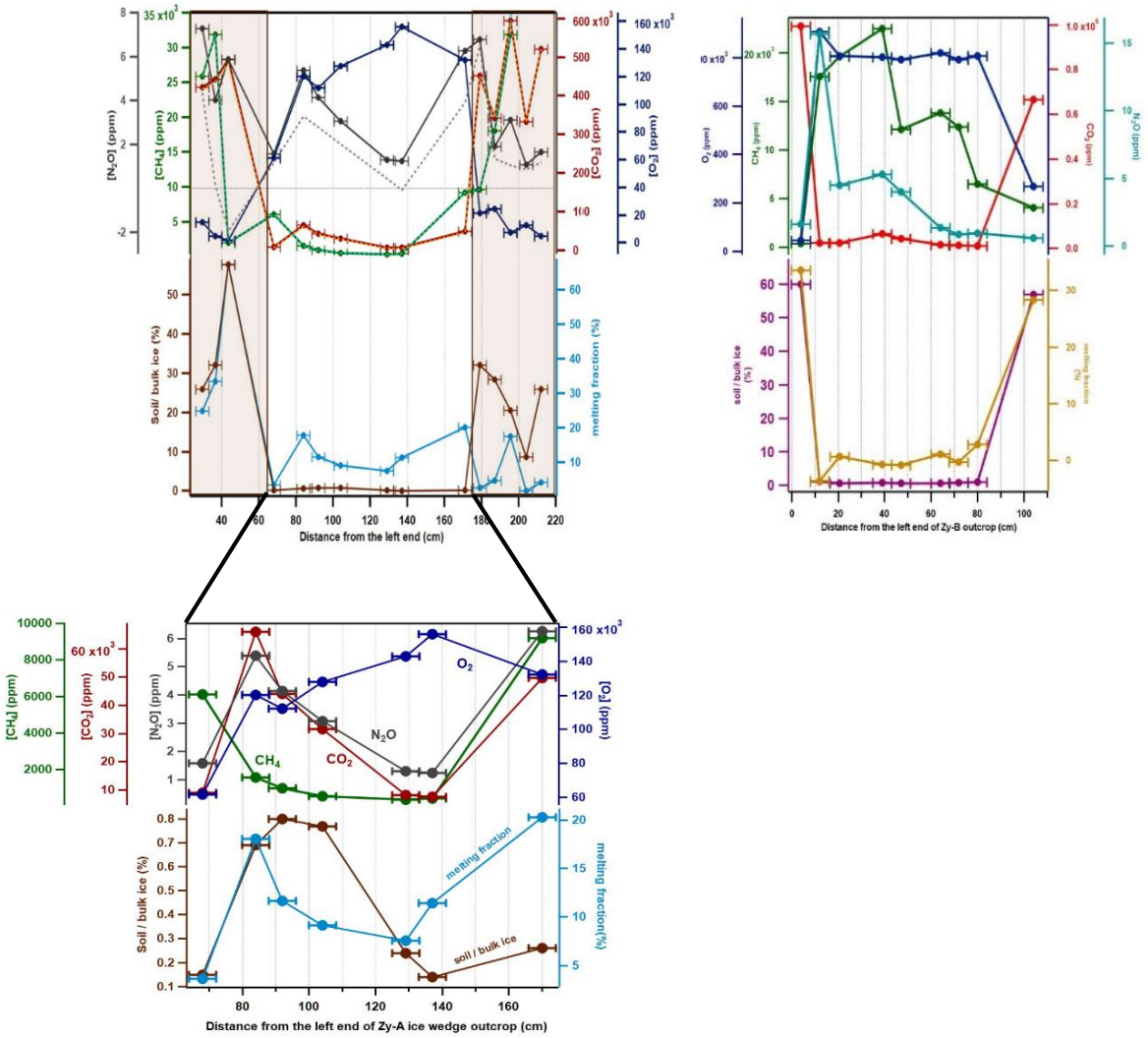

Figure 4. O_2 and greenhouse gas concentration distribution in the Zyryanka ice wedge at A and B site. Each gas concentration was measured simultaneously in the same extracted gas at a given section. Dashed line means the gas concentration that the melting effect is removed. The brown shaded zone in the upper figure indicates texture ice adjacent to ice wedge and the lower one is an enlarged view exclusively for ice wedge part.

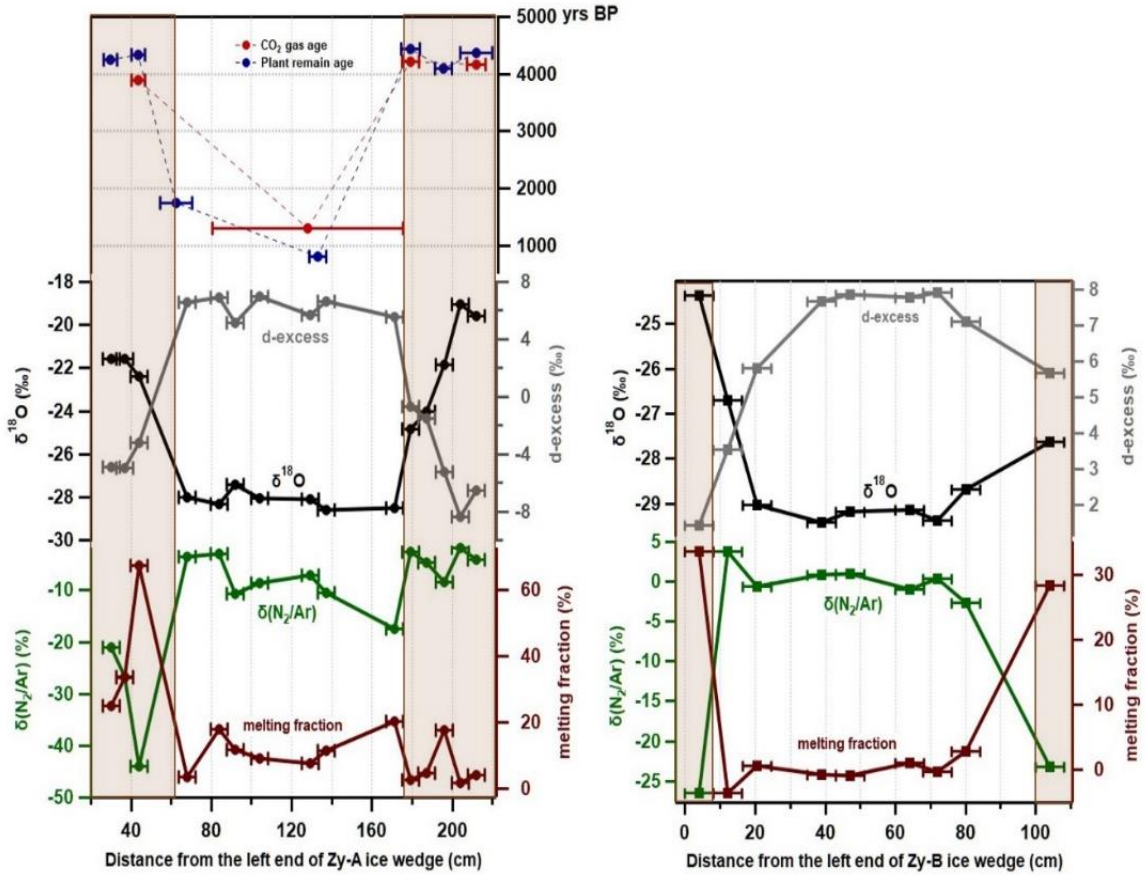

Figure 5. Various chemical parameter and age distribution of the Zyryanka A and B site ice wedge. The brown shade zone indicates the texture ice adjacent to the ice wedge. Age dating for Zyryanka B site ice wedge was not carried out.

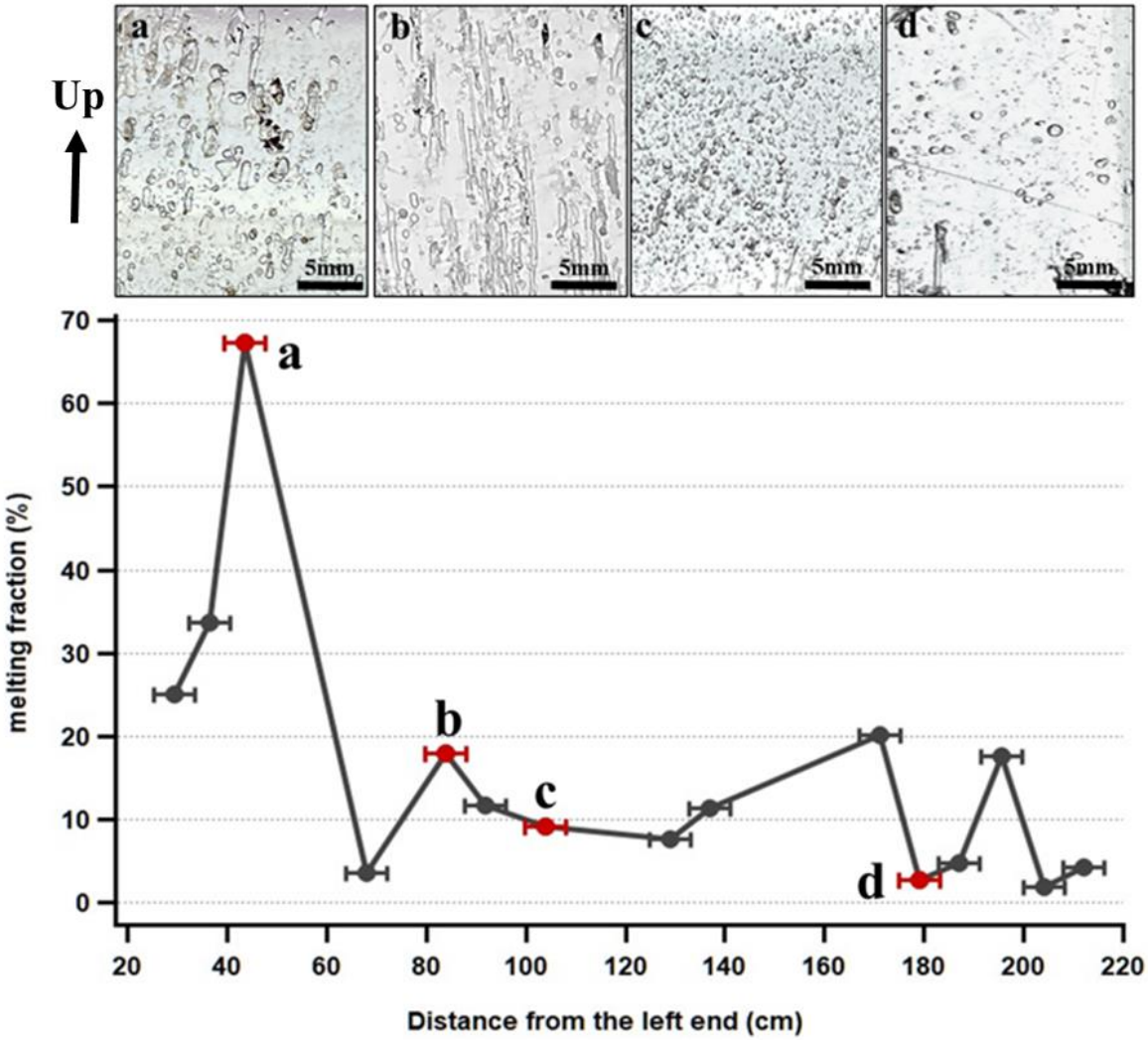

Figure 6. Bubble shapes with different melting degree within the ice wedge from Zyryanka A site (a: Distance from the left 40-47 cm, b: 80-88 cm, c: 100-108 cm, d: 175-183 cm).

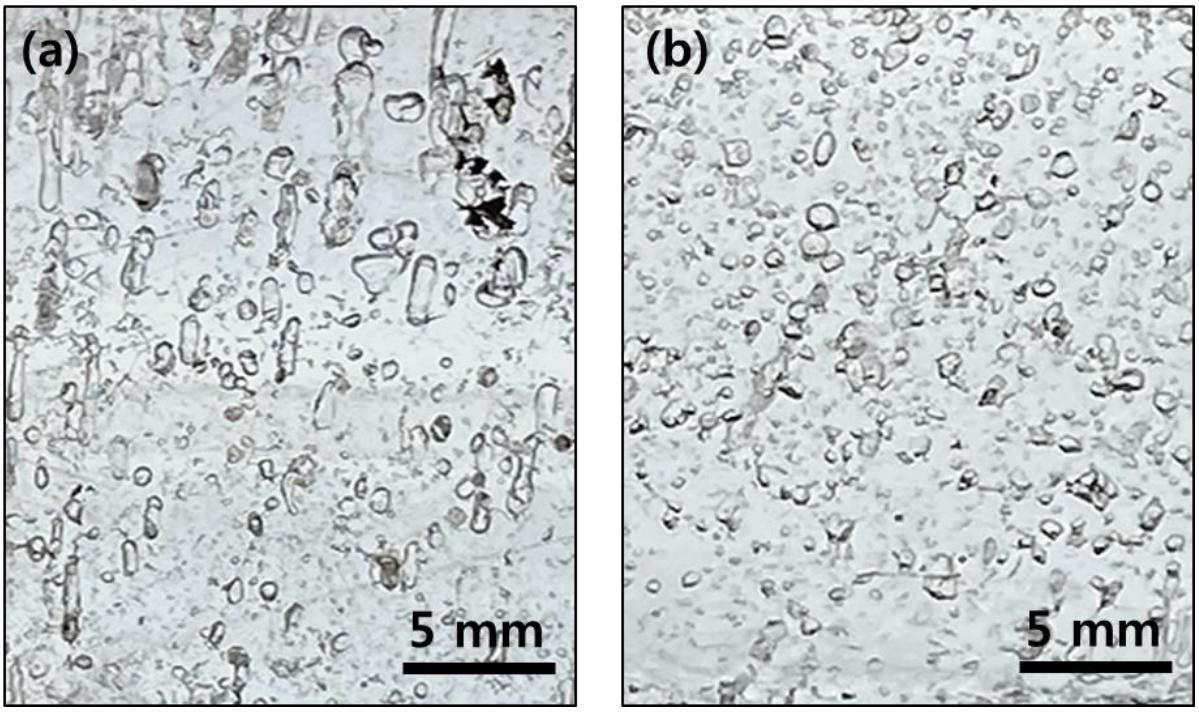

Figure 7. Microphotographs of ice wedge thin sections from Zyryanka A site. (a) 40 - 47 cm ; and (b) 100 – 108 cm. The elongated bubbles appear in areas where unfrozen fractions are relatively high, whereas spherical air bubbles (averaging 1 mm in diameter) can generally be observed in areas with very low unfrozen water fractions.

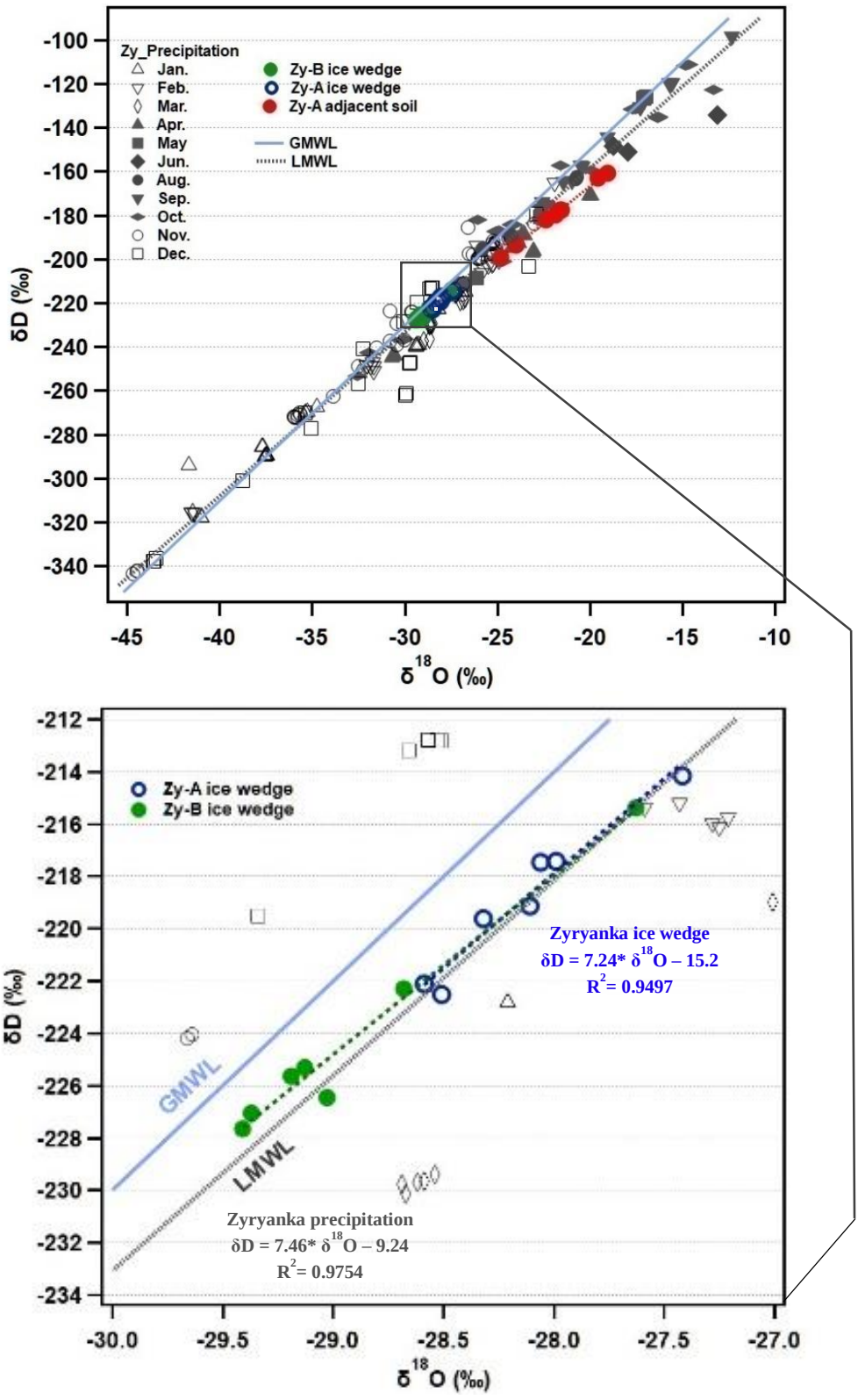

Figure 8. Dual isotope diagram for Zyryanka ice wedge and precipitation from study area. The GMWL (global meteoric water line) is given by $\delta D = 8 * \delta^{18}O + 10$ and LMWL (local meteoric water line) is given by $\delta D = 7.46* \delta^{18}O - 9.24$. The age uncertainty is +/- 30 yrs.

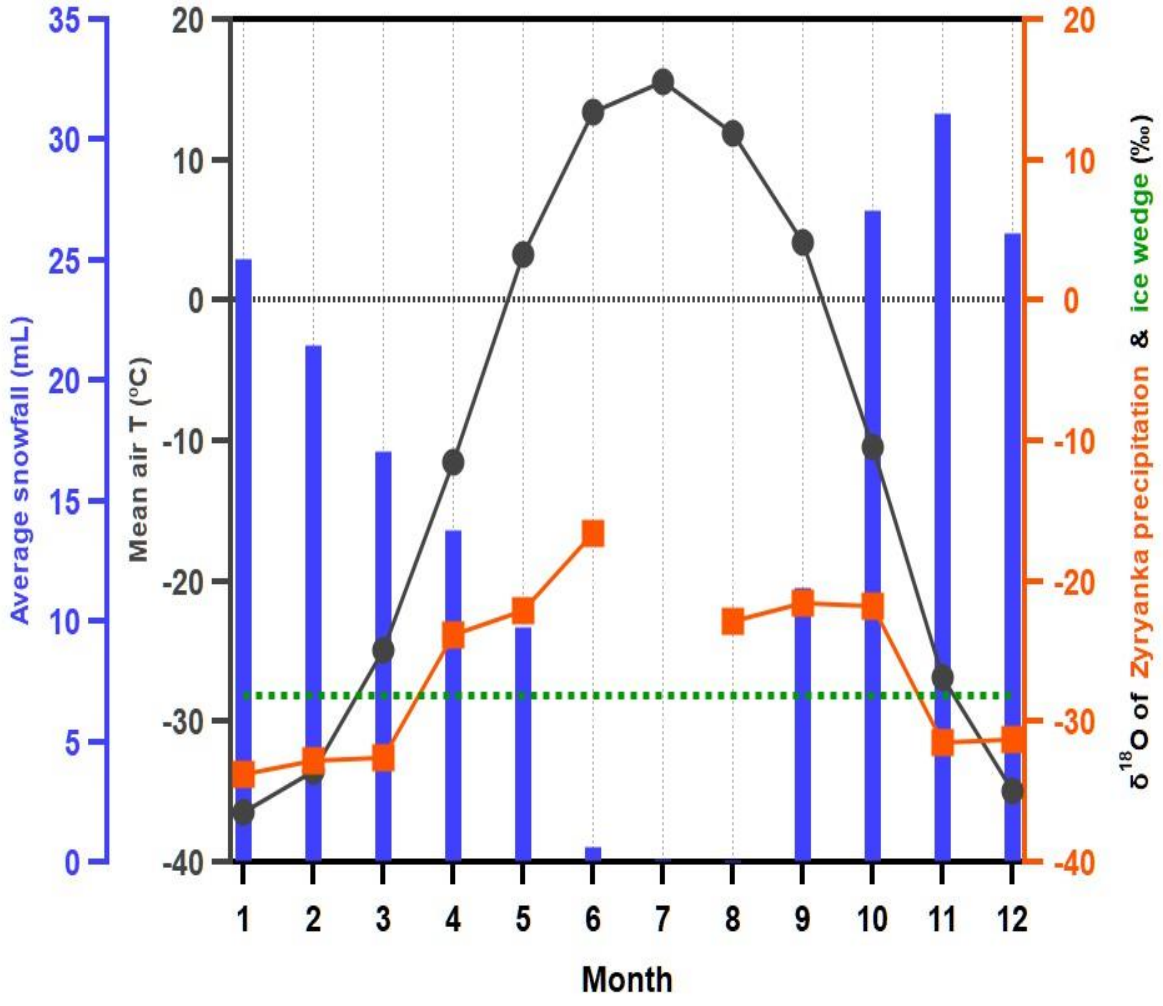

Figure 9. The average snowfall (blue bar) and mean air temperature (black line) of Zyryanka along with $\delta^{18}O$ values of Zyryanka precipitation (orange line) and ice wedge (green dashed line) are shown.

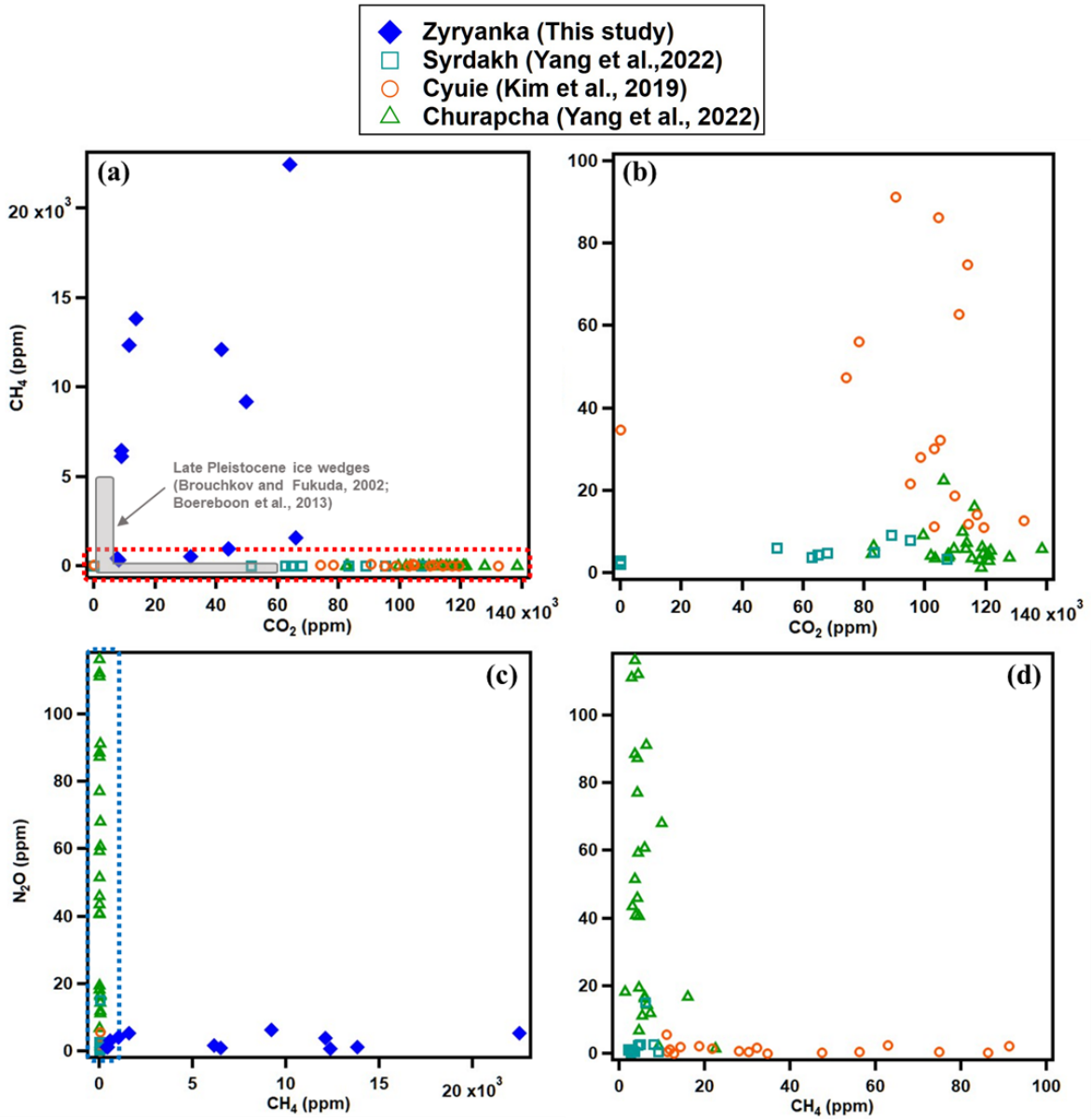

Figure 10. GHGs relationship from different ice wedges of different ages in Siberia. CO_2-CH_4 relationship from (a) all the ice wedges with grey shade box which shows Late Pleistocene ice wedge domain from Brouchkov and Fukuda (2002) and Boereboom (2013), and red dashed box (b) which indicates central Yakutian ice wedges except for Zyryanka ice wedge. CH_4-N_2O relationship from (c) all the ice wedges, and sky blue dashed box (d) which indicates central Yakutian ice wedges except for Zyryanka ice wedge.

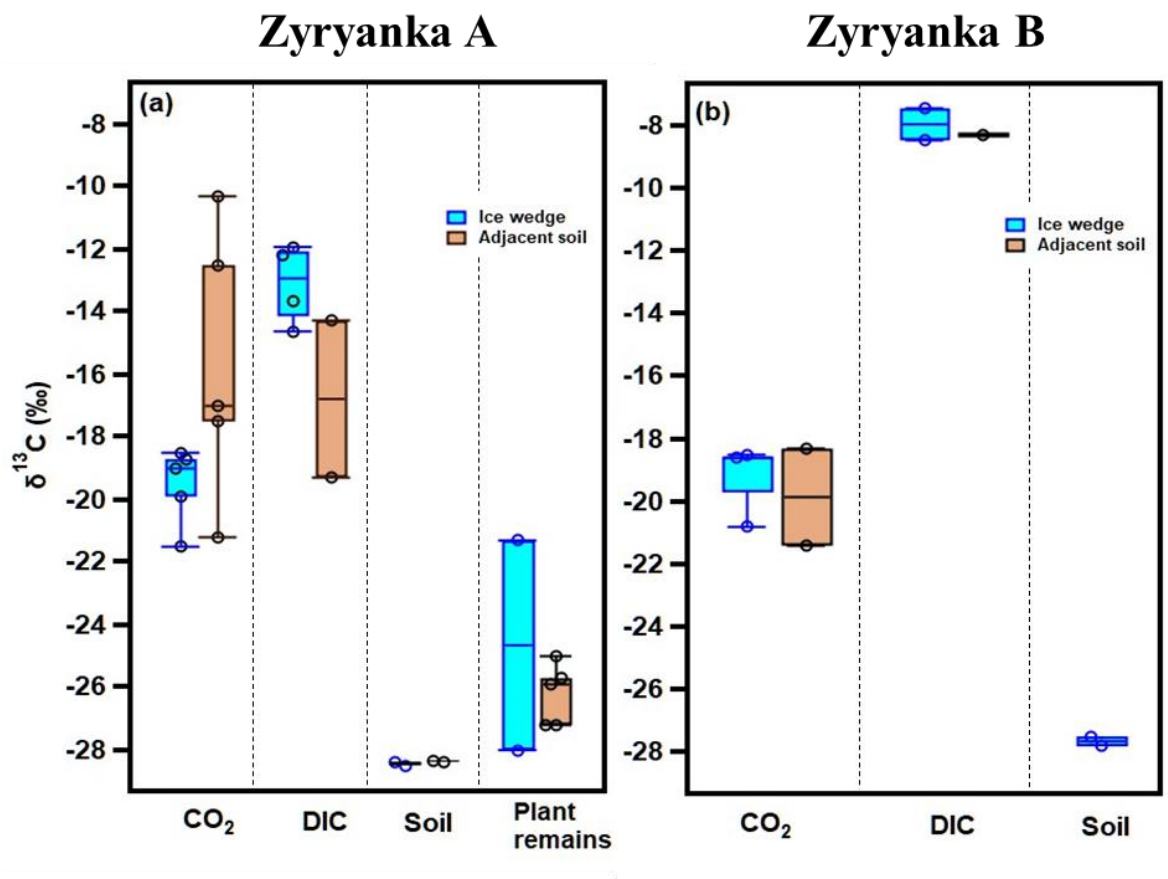

Figure 11. Boxplot of carbon isotope ratio of DIC, soils and plant remains of (a) Zyryanka A site and (b) B site ice wedge samples. Skyblue color indicates that data comes from ice wedge and brown color indicates that data comes from soils adjacent to ice wedge. The open circle symbol represents each measured data value.

List of Tables

Table 1. Radiocarbon age dating results from plant residues and CO_2 gas. Due to the lack of sample amounts, $\delta^{13}C$ was analyzed only for selected samples.

Site	sample	Material	Conventional age	$\delta^{13}C$ (‰)	Source
Zyryanka	Zy_A-W1-A (26-33cm)	Plant residue	4250 +/- 30 BP	-25.7	Adjacent texture ice
	Zy_A-W1-A (40-47cm)	Plant residue	4340 +/- 30 BP	-27.2	Adjacent texture ice
	Zy_A-W1-A (40-47cm)	CO_2	3900 +/- 30 BP	-11.0	Adjacent texture ice
	Zy_A-W1-B (50-75cm)	Plant residue	1750 +/- 40 BP	-21.3	Pure ice wedge
	Zy_A-W1-CDF	CO_2	1300 +/- 30 BP	NA	Pure ice wedge
	Zy-A-W1-E	Plant residue	810 +/- 30 BP	-28.0	Pure ice wedge
	Zy_A-W1-G (175-183cm)	Plant residue	4430 +/- 30 BP	-25.9	Adjacent texture ice
	Zy-A-W1-G (175-183cm)	CO_2	4220 +/- 40 BP	NA	Adjacent texture ice
	Zy_A-W1-G (191-200cm)	Plant residue	4090 +/- 30 BP	-25.0	Adjacent texture ice
	Zy-A-W1-G (191-200cm)	CO_2	4160 +/- 30 BP	NA	Adjacent texture ice
	Zy_A-W1-H (208-216cm)	Plant residue	4370 +/- 30 BP	-27.2	Adjacent texture ice

Table 2. Geochemical data analyzed for the ice wedges at Zyryanka and other site with different age.

Ice wedge location	Zyryanka A site (1290 ± 170 yrs BP)				Zyryanka B site (No age data)				Cyuie (near Yakutsk, Kim et al., 2019) (18130 ± 190 yrs BP)				Syrdakh (near Yakutsk) (26570 ± 160 yrs BP)				Churapcha (near Yakutsk) (20970 ± 80 yrs BP)			
Parameter	Avg.	Min.	Max.	*n*	Avg.	Min.	Max.	*n*	Avg.	Min.	Max.	*n*	Avg.	Min.	Max.	*n*	Avg.	Min.	Max.	*n*
CO_2 (%)	3.08	0.7561	59.39	15	2.68	0.89	6.41	7	10.51	6.93	13.33	33	5.55	0.01	8.71	7	11.2	8.2	13.8	26
CH_4 (ppm)	37789	356.27	273591	15	14917	6485	22471	7	27.4	7.1	86.2	17	6.55	4.14	10.14	7	6.1	1.3	22.5	26
N_2O (ppm)	3.650	1.07	7.27	15	4.62	0.80	15.69	7	0.9	0.07	3.66	17	4.21	0.06	16.88	7	47.3	1.5	116.3	26
Air content(ml/g)	0.025	0.010	0.038	15	0.027	0.0065	0.043	7	0.034	0.028	0.048	22	NA	NA	NA	NA	NA	NA	NA	NA
$\delta(N_2/Ar)$ (%)	-12.95	-43.94	-1.83	15	0.20	-2.74	3.77	7	+2.6	+1.5	+3.2	3	2.60	2.04	3.28	5	NA	NA	NA	NA
$\delta(O_2/Ar)$ (%)	-72.74	-99.06	-37.58	15	-37.26	-65.51	-21.44	7	-98.9	-99.8	-97.4	3	-92.75	-98.18	-90.38	5	NA	NA	NA	NA
$\delta^{18}O_{ice}$ (‰)	-28.14	-28.59	-27.42	15	-28.79	-29.41	-26.70	7	-30.5	-31.5	-29.6	22	NA	NA	NA	NA	NA	NA	NA	NA
δD_{ice} (‰)	-218.92	-222.52	-214.16	15	-223.48	-227.63	-210.05	7	-240.3	-247.0	-235.0	22	NA	NA	NA	NA	NA	NA	NA	NA
d-excess (‰)	+6.21	+5.17	+6.99	15	6.81	3.54	7.90	7	+3.5	+0.4	+5.9	22	NA	NA	NA	NA	NA	NA	NA	NA

Table A1. GHG mixing ratios and $\delta(N_2/Ar)$ and $\delta(O_2/Ar)$ values from Zyryanka ice wedge measured using a wet extraction technique.

sample ID	N_2O	CH_4	CO_2	$\delta(N_2/Ar)$	$\delta(O_2/Ar)$	Material
#	ppm	ppm	%	%	%	
Zy_A-W1-A (26-33cm)	7.27	25919.68	42.21	-20.98	-91.85	adjacent texture ice
Zy-A-W1-A (33-40cm)	4.04	31874.65	44.24	-26.69	-96.94	adjacent texture ice
Zy_A-W1-A (40-47cm)	5.87	2011.79	49.45	-43.94	-99.06	adjacent texture ice
Zy_A-W1-B (64-72cm)	1.59	6123.13	0.91	-3.53	-72.88	Pure ice wedge
Zy_A-W1-C (80-88cm)	5.38	1565.86	6.60	-15.81	-57.1	Pure ice wedge
Zy_A-W1-C (88-96cm)	4.14	984.06	4.40	-10.73	-55.47	Pure ice wedge
Zy_A-W1-D (100-108cm)	3.07	548.58	3.16	-8.57	-46.8	Pure ice wedge
Zy_A-W1-E (125-133cm)	1.31	356.27	0.81	-7.16	-41.37	Pure ice wedge
Zy_A-W1-E (133-141cm)	1.25	425.34	0.76	-10.5	-37.58	Pure ice wedge
Zy_A-W1-F (167-175cm)	6.26	9178.57	4.97	-17.51	-50.03	Pure ice wedge
Zy_A-W1-G (175-183cm)	6.8	9612.87	45.26	-2.67	-83.14	adjacent texture ice
Zy_A-W1-G (183-191cm)	1.92	18076.83	34.29	-4.66	-85.17	adjacent texture ice
Zy_A-W1-G (191-200cm)	3.11	31861.95	59.39	-15.56	-94.2	adjacent texture ice
Zy_A-W1-H (200-208cm)	1.07	273591.9	33.27	-1.83	-85.79	adjacent texture ice
Zy_A-W1-H (208-216cm)	1.67	154703.7	52.14	-4.13	-93.77	adjacent texture ice
Zy_B-LOW-A (0-8cm)	1.57	362.55	99.34	-26.51	-86.57	adjacent texture ice
Zy_B-LOW-A (8-16cm)	15.69	17559.33	2.38	3.77	-65.51	Pure ice wedge
Zy_B-LOW-A (16-25cm)	4.44	19604.81	2.39	-0.63	-38.32	Pure ice wedge
Zy_B-LOW-B (35-43cm)	5.29	22471.05	6.41	0.77	-49.15	Pure ice wedge
Zy_B-LOW-B (43-51cm)	3.96	12100.47	4.17	0.9	-33.63	Pure ice wedge
Zy_B-LOW-C (60-68cm)	1.3	13822.92	1.36	-1.03	-29.07	Pure ice wedge
Zy_B-LOW-C (68-76cm)	0.8	12374.34	1.15	0.35	-21.44	Pure ice wedge
Zy_B-LOW-C (76-84cm)	0.89	6485.17	0.89	-2.74	-23.71	Pure ice wedge
Zy_B-LOW-D (100-108cm)	0.53	4002.23	66.48	-23.17	-83.76	adjacent texture ice

Table A2. Stable water isotope ratio from Zyryanka ice wedge measured at Iwha Womans University in Korea.

Sample ID	$\delta^{18}O$	δD	d-excess	Material
#	‰	‰	‰	
Zy_A-W1-A(26-33cm)	-21.58	-177.55	-4.91	adjacent texture ice
Zy_A-W1-A(33-40cm)	-21.56	-177.49	-4.99	adjacent texture ice
Zy_A-W1-A(40-47cm)	-22.37	-182.12	-3.18	adjacent texture ice
Zy_A-W1-B(64-72cm)	-27.99	-217.41	6.54	Pure ice wedge
Zy_A-W1-C(80-88cm)	-28.32	-219.62	6.93	Pure ice wedge
Zy_A-W1-C(88-96cm)	-27.42	-214.16	5.17	Pure ice wedge
Zy_A-W1-D(100-108cm)	-28.06	-217.47	6.99	Pure ice wedge
Zy_A-W1-E(125-133cm)	-28.11	-219.15	5.71	Pure ice wedge
Zy_A-W1-E(133-141cm)	-28.59	-222.12	6.63	Pure ice wedge
Zy_A-W1-F(167-175cm)	-28.51	-222.52	5.53	Pure ice wedge
Zy_A-W1-G(175-183cm)	-24.83	-199.35	-0.69	adjacent texture ice
Zy_A-W1-G(183-191cm)	-24.01	-193.56	-1.52	adjacent texture ice
Zy_A-W1-G(191-200cm)	-21.84	-179.97	-5.22	adjacent texture ice
Zy_A-W1-H(200-208cm)	-19.06	-160.82	-8.37	adjacent texture ice
Zy_A-W1-H(208-216cm)	-19.58	-163.15	-6.53	adjacent texture ice
Zy_B-LOW-A(0-8cm)	-24.37	-193.56	1.43	adjacent texture ice
Zy_B-LOW-A(8-16cm)	-26.70	-210.05	3.54	Pure ice wedge
Zy_B-LOW-A(16-25cm)	-29.03	-226.44	5.79	Pure ice wedge
Zy_B-LOW-B(35-43cm)	-29.41	-227.63	7.68	Pure ice wedge
Zy_B-LOW-B(43-51cm)	-29.19	-225.62	7.87	Pure ice wedge
Zy_B-LOW-C(60-68cm)	-29.13	-225.30	7.78	Pure ice wedge
Zy_B-LOW-C(68-76cm)	-29.37	-227.05	7.90	Pure ice wedge
Zy_B-LOW-C(76-84cm)	-28.68	-222.30	7.10	Pure ice wedge
Zy_B-LOW-D(100-108cm)	-27.63	-215.39	5.67	adjacent texture ice

Table A3. Average stable water isotope value of monthly precipitation in Zyryanka region from 2017 to 2020 measured at Iwha Womans University in Korea and Kumamoto University in Japan. "n.m." denotes data not measured. Mean air temperature data in Zyryanka region was obtained at "Zyryanka", *Weather and climate*.

Month	$\delta^{18}O$	δD	d-excess	Mean air temperature	#Sample
	‰	‰	‰	℃	
January	-33.77	-258.38	11.75	-36.47	24
February	-32.80	-253.76	8.61	-33.52	22
March	-32.59	-257.03	3.66	-24.87	11
April	-23.84	-193.98	-3.23	-11.47	16
May	-22.13	-172.37	4.66	3.26	10
June	-16.62	-144.57	-11.61	13.41	3
July	n.m.	n.m.	n.m.	n.m.	n.m.
August	-22.89	-177.52	5.63	11.92	4
September	-21.51	-167.36	4.69	4.11	16
October	-21.79	-169.81	4.48	-10.44	29
November	-31.45	-240.62	10.94	-26.83	39
December	-31.24	-245.10	4.79	-34.96	22

Table A4. Major ion concentrations from the Zyryanka ice wedge meltwater samples. "n.a." denotes data not applicable.

Sample ID	Na^+	NH_4^+	K^+	Mg^{2+}	Ca^{2+}	Cl^-	SO_4^{2-}	NO_3^-
#	mg/L	mg/L	mg/L	mg/L	mg/L	mg/L	mg/L	mg/L
Zy_A-W1-A(26-33cm)	2.063	8.703	15.938	n.a.	1.843	15.972	n.a.	n.a.
Zy_A-W1-B(64-72cm)	n.a.	n.a.	n.a.	n.a.	n.a.	1.117	n.a.	n.a.
Zy_A-W1-E(125-133cm)	n.a.	n.a.	n.a.	n.a.	n.a.	1.083	n.a.	n.a.
Zy_A-W1-E(133-141cm)	n.a.	n.a.	n.a.	n.a.	n.a.	1.472	n.a.	n.a.
Zy_A-W1-F(167-175cm)	n.a.	n.a.	n.a.	n.a.	n.a.	0.847	n.a.	n.a.
Zy_A-W1-G(175-183cm)	3.355	9.016	1.683	1.200	3.994	3.133	n.a.	n.a.
Zy_A-W1-H(200-208cm)	n.a.	n.a.	n.a.	n.a.	1.448	1.027	n.a.	4.547
Zy_B-LOW-A(8-16cm)	n.a.	n.a.	3.502	3.857	17.057	1.661	n.a.	n.a.
Zy_B-LOW-B(35-43cm)	n.a.	n.a.	5.107	1.813	5.267	3.964	n.a.	n.a.
Zy_B-LOW-C(60-68cm)	n.a.	n.a.	6.231	1.338	4.205	6.827	n.a.	n.a.
Zy_B-LOW-D(100-108cm)	4.153	n.a.	11.983	21.447	60.870	8.210	26.424	71.583

Table A5. Carbon isotope data and concentration of CO_2 and CH_4 measured by Nagoya University, Japan. "n.m." denotes data not measured.

Sample ID	Measurement	material	CO_2 Conc.	$\delta^{13}C$-CO_2	CH_4 Conc.	$\delta^{13}C$-CH_4
			%	‰	ppm	‰
Zy-A-W1-A	CO_2	adjacent texture ice	34.6	-12.5	n.m.	n.m.
Zy-A-W1-C	CO_2 & CH_4	Pure ice wedge	7.6	-18.7	9,970	-69.6
Zy-A-W1-D	CO_2 & CH_4	Pure ice wedge	5.9	-21.5	3,812	-69.0
Zy-A-W1-G	CO_2	adjacent texture ice	10.0	-21.2	n.m.	n.m.
Zy-A-W1-H	CO_2	adjacent texture ice	40.1	-17.0	n.m.	n.m.
Zy-B-LOW-A	CO_2	adjacent texture ice	8.8	-21.4	n.m.	n.m.
Zy-B-LOW-C	CO_2 & CH_4	Pure ice wedge	0.6	-18.6	12,852	-83.4

Table A6. Average carbon isotope ratio of DIC, soils and plant remains. "n.m." denotes data not measured.

Parameter	Ice wedge location / origin	Zyryanka A site				Zyryanka B site			
		Avg.	**Min.**	**Max.**	***n***	**Avg.**	**Min.**	**Max.**	***n***
δ^{13}C-DIC (‰, w.r.t. VPDB)	*Ice wedge*	-13.09	-14.62	-11.92	4	-7.96	-8.47	-7.45	2
	Adjacent soils	-16.78	-19.29	-14.27	2	-8.3	-	-	1
δ^{13}C-soils (‰, w.r.t. VPDB)	*Ice wedge*	-28.43	-28.49	-28.37	2	-27.67	-27.8	-27.48	2
	Adjacent soils	-28.35	-28.37	-28.33	2	n.m.	n.m.	n.m.	-
δ^{13}C-plant remains (‰, w.r.t. VPDB)	*Ice wedge*	-24.56	-28.0	-21.30	2	n.m.	n.m.	n.m.	-
	Adjacent soils	-26.0	-27.2	-25.0	5	-24.9	-	-	1

Table A7. Summary of precipitation- weighted water isotope values and average air temperature depending on arbitrarily set winter periods. Each of the three right columns represents the difference between the given values.

Arbitrary winter period	**Precipitation-weighted mean $\delta^{18}O$ (‰)**	**Precipitation-weighted mean δD (‰)**	**actual mean air temperature (°C)**	**(Precipitation-weighted mean $\delta^{18}O$) - (Actual mean air temperature)**	**(Precipitation-weighted mean $\delta^{18}O$) - (Ice wedge $\delta^{18}O$)**	**(Ice wedge $\delta^{18}O$) - (Actual mean air temperature)**
Nov. - Mar.	-31.49	-243.96	-28.82	-2.67	-3.03	0.36
Nov. - Apr.	-30.53	-237.73	-25.05	-5.48	-2.07	-3.41
Dec. - Feb.	-31.96	-248.12	-32.76	0.79	-3.50	4.30
Dec. - Mar.	-32.00	-349.22	-40.96	-1.74	-3.54	1.80
Oct. - Apr.	-28.40	-221.39	-22.82	-5.58	0.06	-5.64